SUPRAMOLECULAR HOST-GUEST CHEMISTRY IN DESIGN OF IONOPHORES FOR POTENTIOMETRIC CHEMFET SENSORS

by

GRACE M. KUHL

A DISSERTATION

Presented to the Department of Chemistry and Biochemistry
and the Division of Graduate Studies of the University of Oregon
in partial fulfillment of the requirements
for the degree of
Doctor of Philosophy

September 2022

DISSERTATION APPROVAL PAGE

Student: Grace M. Kuhl

Title: Supramolecular Host-Guest Chemistry in Design of Ionophores for Potentiometric ChemFET Sensors

This dissertation has been accepted and approved in partial fulfillment of the requirements for the Doctor of philosophy degree in the Department of Chemistry and Biochemistry by:

Amanda Cook	Chairperson
Darren Johnson	Advisor
Mike Haley	Core Member
Keat Ghee Ong	Institutional Representative

and

Krista Chronister	Vice Provost for Graduate Studies

Original approval signatures are on file with the University of Oregon Division of Graduate Studies.

Degree awarded September 2022

DISSERTATION ABSTRACT

Grace M. Kuhl

Doctor of Philosophy

Department of Chemistry and Biochemistry

September 2022

Title: Supramolecular Host-Guest Chemistry in Design of Ionophores for Potentiometric ChemFET Sensors

Potentiometric sensors are a viable technology for monitoring aqueous anion concentration in real-time, a key process in numerous applications. However, selectivity in such systems remains challenging in part due to water's polarity. Comparison between solution-state binding, and potentiometric calibrations is needed to tune ionophore design and optimize sensor performance.

The work reported in this dissertation explores the use of host-guest chemistry by incorporating synthetically tailored receptors into polymer membrane-coated insulated gate field effect transistors. Potentiometric calibrations and interference studies yield data about reusability, sensitivity, detection limit, and selectivity. In the case of barbituric acid, devices were prepared based on membranes containing Hamilton-type receptors as the ionophore. They exhibit near Nernstian sensitivity and demonstrate utility of Hamilton receptors within polymer membranes for potentiometric detection of barbiturates in water. This work also investigates the effects of receptor preorganization on sensor performance and compares these effects to those observed for similar receptor systems in solution.

Using a similar approach, this work also investigates sensor materials for

hydrosulfide. We prepared and evaluated devices based on a nitrile butadiene rubber without ionophore, only containing lipophilic salt as a chemical recognition element applied to an insulated gate field-effect transistor surface. The sensors have quick and reversible responses and selectivity over some thiol-containing species.

To improve HS^- sensor performance, we synthesized a novel bambusuril macrocycle to employ as the membrane ionophore. This yielded detection limits below 0.5 mM and selectivity over chloride and cysteine. Continuing to study the utility of bambusuril macrocycles as ionophores, we begin an investigation with the Hofmeister series suing bambus[6]uril-doped membranes. Thus far, we find that in the absence of ionophore, bromide disrupts the expected response with a lower detection limit than iodide and perchlorate. When a bambus[6]uril macrocycle is incorporated as the ionophore, detection limits dropped at least one order of magnitude for all anions tested with the exception of bromide. To further elucidate a trend imparted by the ionophore, further experiments should be performed across the spectrum of the Hofmeister series.

This dissertation includes both co-authored unpublished material and previously published work.

CURRICULUM VITAE

NAME OF AUTHOR: Grace Marie Kuhl

GRADUATE AND UNDERGRADUATE SCHOOLS ATTENDED:

University of Oregon, Eugene
Creighton University, Omaha

DEGREES AWARDED:

Doctor of Philosophy Chemistry, 2022, University of Oregon
Master of Science, Chemistry, 2019, University of Oregon
Bachelor of Science, Chemistry, 2018, The Pennsylvania State University

AREAS OF SPECIAL INTEREST:

Wearable sensors
Potentiometric sensors
    Field effect transistors
    Ionophore design
Organic macrocycle synthesis
Organic macrocycle characterization
    Nuclear magnetic resonance spectroscopy
    Mass spectrometry
    Crystallography

PROFESSIONAL EXPERIENCE:

Graduate Research Assistant, Department of Chemistry and Biochemistry, University of Oregon, 2019-2022

Graduate Teaching Assistant, Department of Chemistry and Biochemistry, University of Oregon, 2018-2019

GRANTS, AWARDS, AND HONORS:

First Year Merit Award, University of Oregon, 2018

Baumann Scholar, Creighton University, 2018

Clare Boothe Luce Scholar, Creighton University, 2017-2018

PUBLICATIONS:

Sherbow, T. J., Kuhl, G. M., Lindquist, G. A., Levine, J. D., Pluth, M. D., Johnson, D. W., & Fontenot, S. A. **2021**. *Sensing and Bio-Sensing Research*, *31*, 100394.

Kuhl, G. M., Seidenkranz, D. T., Pluth, M. D., Johnson, D. W., & Fontenot, S. A. **2021**. *Sensing and Bio-Sensing Research*, *31*, 100397.

ACKNOWLEDGMENTS

I am incredibly lucky to have been endlessly supported by educators, mentors, friends, and family. Without you, this success would not have been possible. First, I must extend my biggest thanks to my advisor, Dr. Darren Johnson. You are an integral part of my growth as a chemist and young professional. You have nudged me through this degree, letting me set my own goals and rules. Thank you for your patience, counsel, and faith in my ability to handle a full plate.

Thank you to my mentors- you've left an impact on the scientist and woman I am becoming. To Dr. Eric Villa for instilling me with a love for research and pretty crystals, Dr. Sean Fontenot and Dr. David Dobberpuhl for teaching me more about life than chemistry, and Dr. Shula Jaron for her professional guidance in my final year of graduate school. To my former student mentors, Drs. Jeremy Bard, Hazel Fargher, and Jordan Levine, thank you for your help in lab, writing, navigating the program, and showing me life can go on after graduate school. Thaís de Faría, thank you for always putting a smile on my face and answering my lab questions. Hannah Bates, thank you for the bridge runs, belly laughs, game nights, and friendship during this entire program. Seeing your face in and out of lab is a constant source of joy. The rest of the DWJ lab- especially Willow Davis, Doug Banning, Alex Rosen and Luca Zocchi, thank you for making a lab feel like a home.

To my friends outside of chemistry- Samantha Jarman, Callie McDonald, Beth Martin, Denae Reeves, Matt Strigenz, Michael Mimlitz & Ian Gallaher, you always bring me back to reality when I spiral into a deep dark chemistry hole. Thank you for keeping my sanity intact and making sure I have some fun. Your friendship means the world to me.

Benjamin McDowell, there isn't enough space to cover how much your support means to me. You are my soux chef, fiercest card game opponent, and best friend. You taught the benefits of going with the flow and helped bring the delightful creature we know as Bear into my life. Thank you for listening to my rants, always keeping me caffeinated, and for your loving patience.

Finally, thank you to my family for supporting me throughout my entire academic career. You've been there to celebrate the highs and pick me up after the lows. Thank you for all the phone calls, plane tickets home, and reminders that I am loved.

Dedicated to the my family, friends, and future women in chemistry.

TABLE OF CONTENTS

Chapter Page

LIST OF FIGURES

LIST OF TABLES

LIST OF SCHEMES

Scheme Page

CHAPTER I

INTRODUCTION

I am the primary and only author of this chapter.

Background and Motivation

Importance of anion detection in water

Sensing of aqueous anions is key to advancing fields such as healthcare[1], agriculture,[2, 3] and environmental remediation.[2, 4] Despite the global abundance of water, monitoring its anionic contents remains challenging due to water's unique polar properties[5], including complex anionic geometry and strong ion hydration energies.[6, 7] In the applications above, current technologies used for anion quantification feature chemical sensing systems such as Raman spectroscopy[8], colorimetry[9], and gas chromatography-mass spectrometry[10]. Although these methods provide an accurate snapshot of chemical information and sub-parts per trillion (ppt) detection limits, they require complex sample preparation, instrumentation, and training without the benefit of real-time data.[8] As a result, there has been a multidisciplinary effort between scientists and engineers to develop continuous anion sensors for simple and consistent water analysis.

Chemical sensors are defined as devices which intake chemical information, such as concentration, and translate it into a measurable analytical signal.[11, 12] Chemical sensors employed in sensing devices are preferably selective and quick, acquiring and relaying information continuously. There are two general components to a chemical sensor: a receptor and a transducer.[13] Receptors exist at the interface of the sensor and the sample, converting chemical information to measurable energy using physical, chemical, or biochemical recognition. The

transducer takes this energy and further transforms it to analytical information (Figure 1.1).[11, 14] This dissertation focuses on developing sensor membrane materials to improve sensitivity and selectivity in electrochemical, specifically potentiometric, sensors employed in aqueous sample solutions.

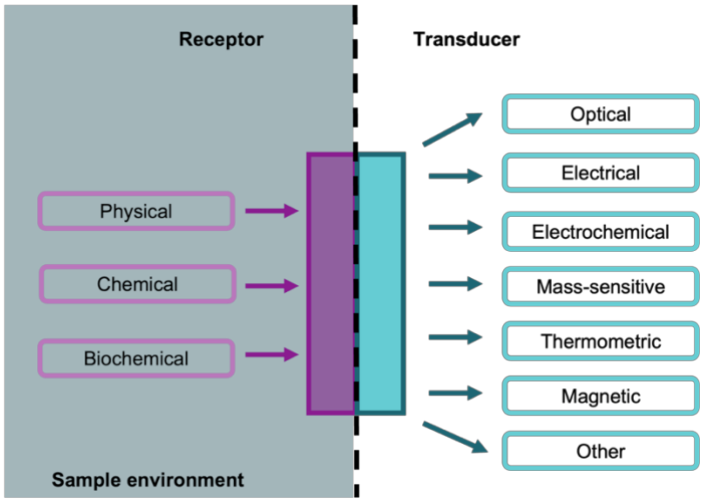

Figure 1.1 A simplified depiction of the combinations of transducers and receptors that comprise the broad field of chemical sensors.

Electrochemical sensors are defined as producing voltage, current, or resistance based on the interactions at an electrode-electrolyte interface.[14, 15] In general, electrochemical sensors are valued for quick response times, no sample pretreatment, sensitivity [16], and cost-effectiveness.[17] The two commonly recognized categories of electrochemical sensors are amperometric and potentiometric.[18] Of these, potentiometric sensors are miniaturizable[6], inexpensive to produce, and have straightforward instrumentation.[19] These attributes are attractive for applications in biosensing,[20] precision agriculture,[3, 21] and environmental remediation.[22] Therefore, there is much interest in improving the efficacy of potentiometric sensors.

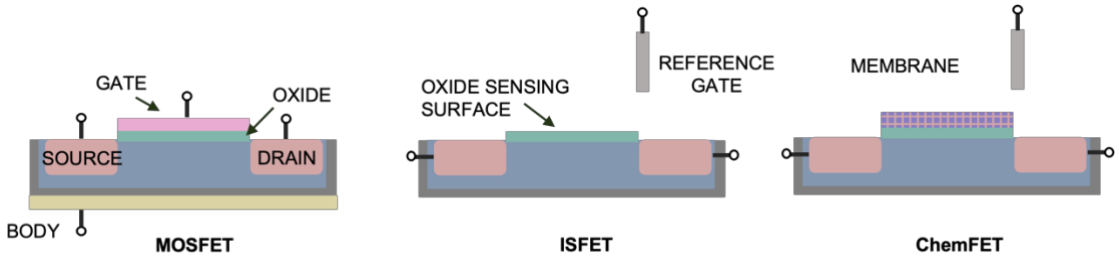

Figure 1.2 Cross section of FET devices illustrating locations of electrical circuit contacts.

Chemically selective field effect transistors

Field effect transistors (FETs) are a three terminal electronic device employed widely in the technology industry and can be a base for label-free chemical sensors.[23] Metal-oxide semiconductor FETs (MOSFETs) serve as the base architecture for potentiometric ion sensitive FETs (ISFETs), both of which contain a semiconductor source and drain terminal as shown in Figure 1.2.[24] The ISFET replaces the metal gate with a reference electrode combined with a sensing surface layer, such as SiO_2, that is sensitive to H^+.[25] The ISFET response is attributed to the oxide's pH-dependent, reversible surface protonation.[26-28] Modification of the sensing surface to impart selectivity towards a target chemical (gases, ions, and biomolecules) results in a chemically selective field effect transistor (ChemFET).[24, 28, 29]

Introduced in 1975 with K^+ as the analyte,[30] ChemFETs have evolved into a microscale, low power consuming, and label-free option for ion monitoring.[28] The main differences between ChemFETs and other potentiometric sensors, mainly ion-selective electrodes, is that the sensing surface is in contact with a solid rather than an electrolyte and there is no internal reference,[24] which can offer added durability and stability during measurements (Figure 1.3).[31]

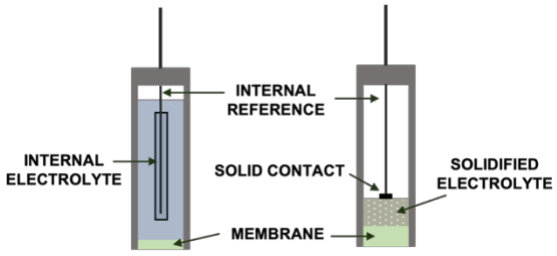

Figure 1.3 Representation of liquid (left) and solid (right) contact ion-selective electrodes.

The internal circuitry of an ISFET/ChemFET comprises an n/p semiconductor pair, similar to that of a MOSFET.[27] In this work, the n-type source and drain are separated by a p-type semiconductor substrate. Current flows source to drain through a depletion region that forms when a minimum voltage is applied. The magnitude of this region is influenced by the field effect at the gate sensing surface (Figure 1.4).[23] In ISFETs/ChemFETs, the sensing surface is in direct contact with an aqueous solution.[30, 32] If the sensing surface is coated in a polymer-based ion selective membrane, the ChemFET interface can be modeled like an ISE.[28, 33]

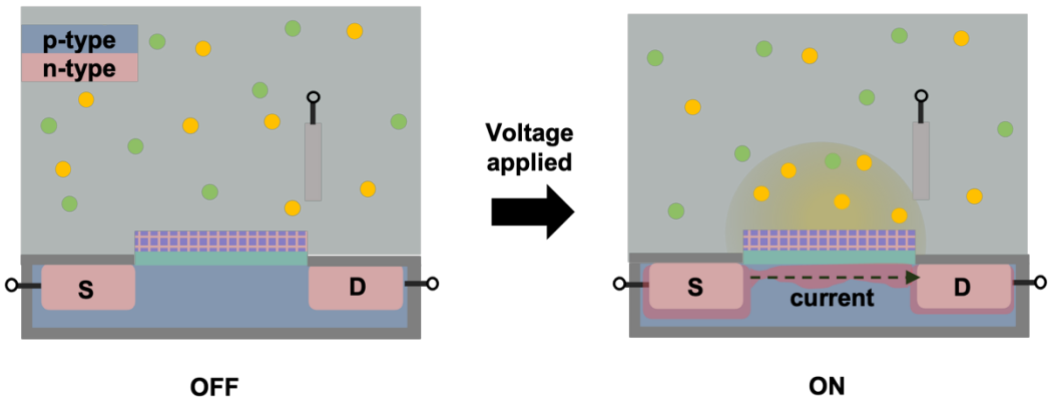

Figure 1.4 In an electrolyte solution (yellow anions & green cations), applied voltage and an external field effect at the sensing surface (purple checkers) form a depletion region at the P/N junction. This allows current to flow source to drain.

Ion-selective polymer membranes

ChemFETs and traditional ion selective electrodes have a potential voltage related to the interface of a polymer membrane with an electrolyte sample solution.[11, 33] The total potential of a cell can be described using the Nikolsky-Eisenman equation:[34]

$$(1.1) \quad E_{cell} = E_{cons} + \frac{2.303\,RT}{z_A F} log\,(a_A + K_{A,B}\, a_B^{z_A/z_B})$$

Where E_{cons} is the sum of all constant potentials within the cell. Ions A and B have activities a_A and a_B, $z_A$and z_B are ion charges. R is the ideal gas constant, T is temperature in Kelvin, and F is Faraday's constant. Finally, $K_{A,B}$ is an experimentally determined selectivity coefficient that can be determined by:

$$(1.2) \quad K_{A,B} = \frac{a_A}{a_B^{z_A/z_B}}$$

Where a_A and a_B are the activities of A and B at their respective limits of detection determined with potentiometric calibration and the fixed interferent method.[34, 35] Note that Equation 1.1 can be simplified in the absence of an interferent to:

$$(1.3) \quad E_{cell} = E_{cons} + \frac{2.303\,RT}{z_A F} log\,(a_A)$$

The above is recognizable as the Nernst Equation. Looking back to Equation 1.2, sufficient selectivity is achieved when $K_{A,B} < 1$. However, as mentioned above, anions have inherent

challenges to their detection. Supramolecular chemistry can serve as a useful tool in designing ionophores that preferentially interact with the target analyte of interest over interferents.

Translating host-guest chemistry to ionophore design

One means of imparting chemical selectivity is to iterate on principles established by supramolecular host-guest chemistry.[36, 37] The crossover with potentiometric sensors exists in hosts, or receptors, that selectively bind to a charged guest.[38, 39] A receptor refers to the macromolecule in free solution and called ionophores when incorporated into a membrane. Both are built from molecular units arranged in a complementary geometry for a specific target.[38, 40] In this design, there are some key similarities and differences to identify in order to strive towards using existing knowledge to progress ionophore design.

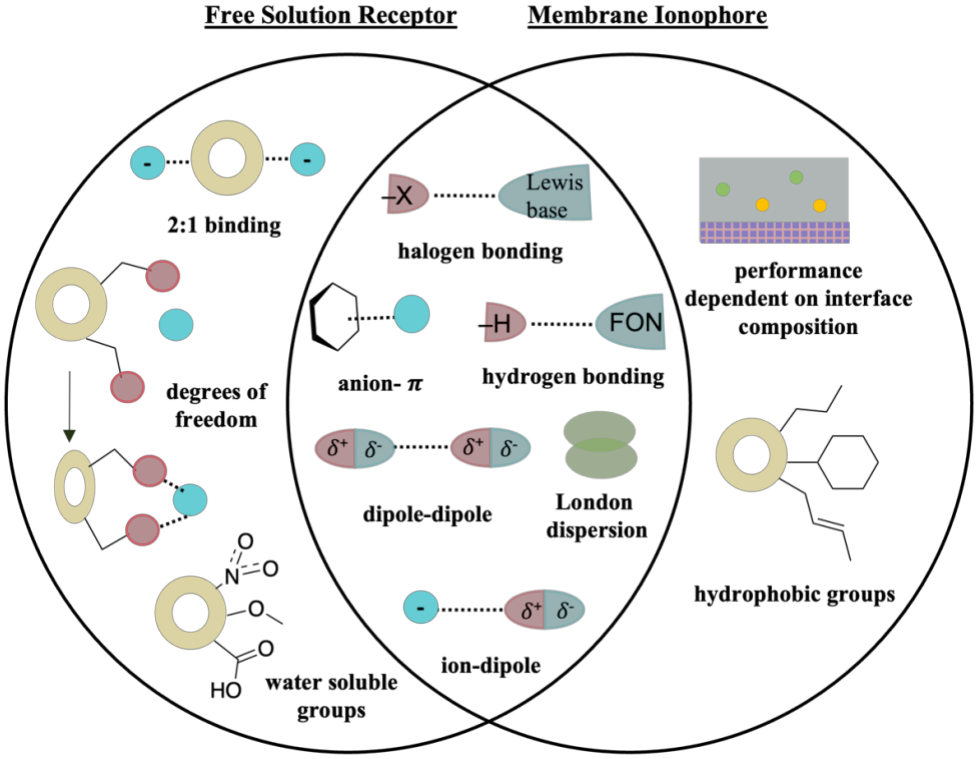

Figure 1.5 Visual Venn-Diagram that highlights the shared use of noncovalent interactions as well as structural considerations.

Receptors and ionophores tune selectivity using strategically placed noncovalent interactions, like hydrogen bonding and π interactions (see Figure 1.5). The sum of these must be strong enough to overcome an ion's hydration energy yet remain reversible to enable dynamic sensing.[36,41] In addition to selectivity, solubility is a key attribute in aqueous host-guest chemistry.[39] This is achieved in receptors through implementation of polar or charged functional groups in contrast to hydrophobicity necessary in ionophores to combat membrane leaching.[6] A final important difference to highlight is in the mobility of receptors vs. ionophores. In free solution, receptors can rotate through space, bind 2:1 with an analyte, and change conformation to optimize stabilizing noncovalent interactions. There are a number of receptors that have been successfully integrated as ionophores, such as triazolophanes, calixarenes,[42] and most recently, bambusurils[22] (See Figure 1.6). With the tools gathered from supramolecular host-guest chemistry, it is possible to incorporate a potentiometric platform for anion detection.

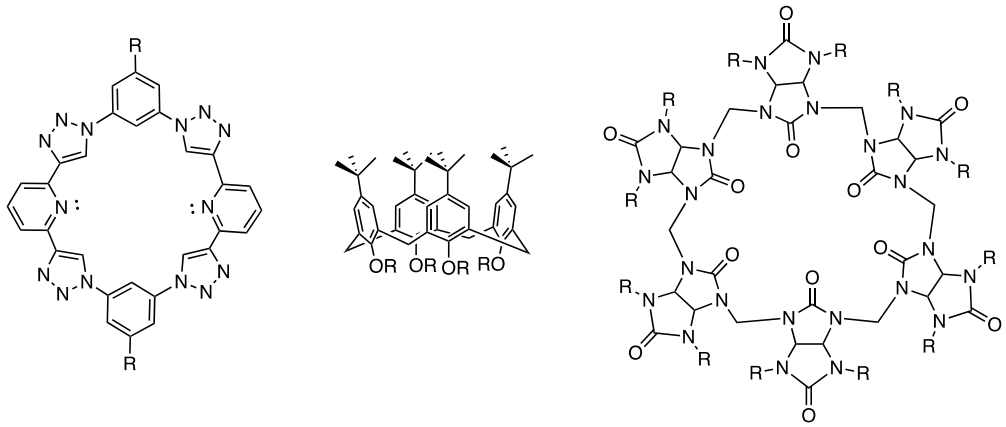

Figure 1.6. From left to right: triazolophane incorporated into ISE for halides,[43] calix[4]arene macrocycle, bambus[6]uril macrocycle.

Dissertation Overview

Above, we introduce the idea that ionophores can be built with a binding pocket containing complementary noncovalent interactions, similar to a host-guest receptor. When integrated with chemically selective field effect transistors (ChemFETs), these ionophores interpret analyte concentration as a voltage response. This thesis explores host-guest inspired ionophores beginning in Chapter II with employing a Hamilton receptor as a ChemFET ionophore to detect barbituric acid in buffered water. Chapter III targets the hydrosulfide (HS^-) anion with commercially an available ion exchanger and an alternative reference electrode for ChemFET measurements is identified. Chapter IV revisits detection of HS^- with a bambusuril macrocycle as the ionophore and begins a potentiometric investigation of the Hofmeister series. Finally, Chapter V contains concluding remarks and potential future directions for ionophore exploration.

Bridge to Chapter II

The preceding chapter introduced chemical sensors, specifically potentiometric sensors, as a viable tool for anion recognition in water. Integration of supramolecular chemistry can allow potentiometric sensors to be used for specific analyte recognition. The following chapters will illustrate successful use of potentiometric sensors to indicate target analyte concentration through use of supramolecular receptors. The measure of success of the receptors in ChemFETs was verified using potentiometric calibration and fixed interferent methods. Ionophore preorganization impact on sensor performance will be discussed. The relevant figures of merit, including sensitivity, selectivity, and detection limit will be outlined and evaluated in numerous cases in Chapters II, III and IV.

CHAPTER II

POTENTIOMETRIC MEASUREMENT OF BARBITURIC ACID BY INTEGRATION OF HAMILTON-TYPE RECEPTORS INTO CHEMFETS

This chapter was previously published as Kuhl, G. M., Seidenkranz, D. T., Pluth, M. D., Johnson, D. W., & Fontenot, S. A. Sensing and Bio-Sensing Research Potentiometric measurement of barbituric acid by integration of supramolecular receptors into ChemFETs. *Sensing and Biosensing Research.* **2021**, *31*, 100397.

Introduction

Methods for anion and cation detection in water are crucial due to the diverse roles that ions play in biological and environmental systems.[1-3] The introduction of synthetic ions, such as pharmaceuticals and their metabolites, into the environment may upset the ecosystems in which they accumulate.[4,5] For example, diphenhydramine, or DPH (Figure 2.1), is a common antihistamine.

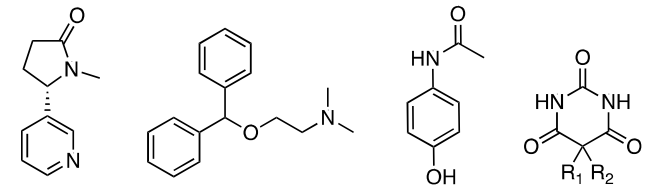

Figure 2.1 Examples of known ionic pharmaceutical pollutants used as a sleep aid and provides symptom relief for hay fever and motion sickness.[6] Recent studies have revealed the presence of DPH in municipal biosolids used to fertilize agricultural soil.[7,8]

Due to the proton accepting amino group, DPH exists as a cation at conditions investigated in this work. Barbiturates, a class of small molecule pharmaceuticals derivatized from barbituric acid (several of which are anionic at neutral pH) are also designated as environmental pollutants due to their harmful effects on local wildlife.[5,9] Work investigating barbiturate degradation in natural waters revealed persistent µg/L concentrations and little breakdown in aqueous environments over the span of 9 months.[5] Detection of such substances continues to be a crucial component of environmental monitoring and remediation.

Electrochemical detection methods for ionic pollutants, such as barbiturates, can employ chemical receptors with high affinity and specificity for the target analyte to induce a measurable response.[1,10,11] For many potentiometric detection methods, receptors for the anion or cation of interest are often incorporated into polymeric ion selective membranes (ISM).[10] Design strategies for receptors targeting cations in aqueous environments are well-established, but anion recognition strategies are comparatively under-developed.[1] Charge to size ratio, strong solvation, and vastly ranging degrees of hydrophilicity/hydrophobicity contribute to the elusive nature of selective anion recognition.[1,12-14] There is a great deal of interest and effort in developing anion-selective

chemistries, and the fruits of these efforts have been diversity receptors, design strategies, and sensing methods for targeting anions.[1]

One approach to developing selective anion receptors is to utilize supramolecular host-guest chemistry in which the guest is targeted by various noncovalent intermolecular interactions.[14] Hydrogen bonding, ion pairing, electrostatic forces, hydrophobic interactions, and halogen bonding[1,15,16] are common tools for construction of complementary binding architectures. Using these tools, a plethora of scaffolds have been developed and derivatized.[12] Key examples include, but are not limited to, foldamers,[17] porphyrins,[15] rotaxanes,[18] and cyclodextrin analogues.[19]

In 1987, Hamilton and co-workers introduced a novel motif for the recognition of barbiturates. Hamilton's acyclic receptors participate in 1:1 binding with barbiturates through six strong and directional hydrogen bonds forming "ADA-DAD"-type motifs within the binding pocket on both sides of the guest (A=hydrogen bond acceptor, D=hydrogen bond acceptor, see Figure 2.2).[20]

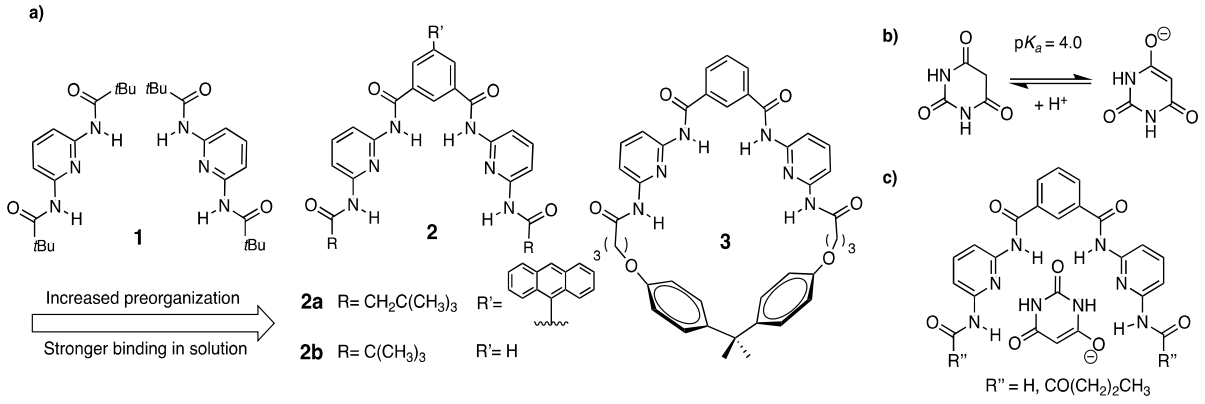

Figure 2.2 a) Hamilton receptors from McGrath et al. (2014, Ref. 21) showing different degrees of preorganization; b) unsubstituted barbituric acid; c) illustration of Hamilton's original acyclic receptor and its association with barbituric acid via complementary HB donor and receptor pairs.

This well-studied scaffold can be tuned for the recognition of other molecules which have the appropriate donor-acceptor motif. Examples include cyanuric acid, uracils, thymines, glutarimides, succinimides, and dipyridine-2-ylamines.[21] Reported applications of Hamilton-type receptors include catalysis, optoelectronic materials, polymer formation, and nanoparticle self-assembly.[21-23] However, barbiturate derivatives continue to be ideally suited to recognition by Hamilton-type receptors.

The conjugate base of barbituric acid is an anion and is therefore suitable for detection by potentiometric methods. By transducing a chemical reaction to a measurable electrical signal, potentiometric sensors provide continuous detection of a target analyte. Chemically sensitive Field Effect Transistors (ChemFETs) can be made to accomplish this by applying an ISM to modulate the interaction between the gate surface and a sample environment. Simply put, the potential response for a ChemFET is the sum of multiple interfacial potentials between the gate electrode and the FET substrate. When constructed correctly, the only variable potential among these is that between the ISM and solution environment. The magnitude of this potential drop is dependent on the activity of the target analyte in solution. Therefore, one can relate the change in ion activity to the change in potential as described by the Nernst equation.

Various spectrophotometric and electroanalytical methods have been reported for BBA measurement.[24-28] There are not, to our knowledge, any potentiometric methods for direct determination of BBA or its derivatives. We report our ChemFET system of having an optimized detection limit of less than 0.064 mmol compared to 0.004 mmol reported for amperometric[24] and 0.012 mmol for voltammetric[25] methods. While the other techniques have excellent LOD, they commonly require multi-electrode set-ups, the addition of additional chemicals, and complex instrumentation. Our potentiometric sensors have the advantage of facile operation and minimal

sample preparation while maintaining substantial sensitivity using simple, well-established electronics and a conventional multimeter.

Experimental

Reagents and solutions

Unless otherwise indicated, all reagents were used as received. Anhydrous, deoxygenated solvents were collected from a Pure Process Technologies solvent purification system. Chromatographic purification was performed using a Biotage automated flash chromatography purification system. Nitrile Butadiene Rubber (Nipol DN401LL) was purchased from Zeon Chemicals. All other chemicals were purchased from Fisher Scientific, Sigma-Aldrich, or Tokyo Chemical Industry. River water was obtained from the Willamette River in Eugene, Oregon, and the samples were not filtered or treated prior to use. Turbidity was measured at 4.1 NTU, dissolved oxygen content of 10.9 mg/L. Synthetic urine was obtained from Carolina Biological.

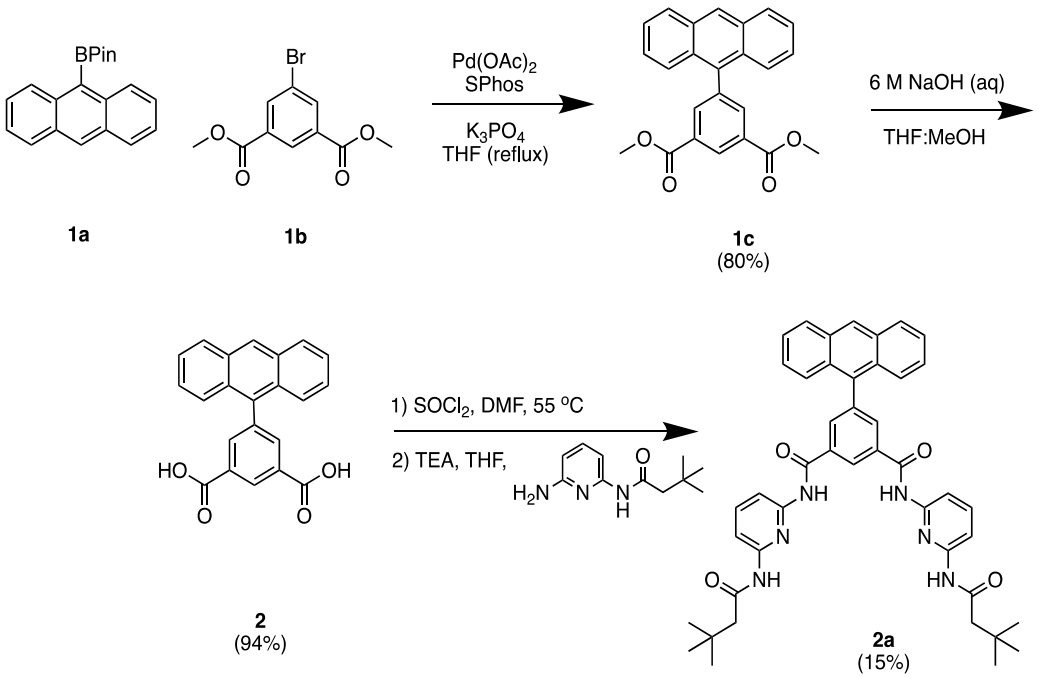

Figure 2.3 Synthetic scheme for receptor 2a.

Receptor synthesis and characterization

Dimethyl 5-(anthracen-9-yl)-isophthalate (**1c***)* was prepared via an adaptation of a reported procedure.[29] To a solution of $Pd(OAc)_2$ (22 mg, 0.10 mmol) in degassed THF was added SPhos (118 mg, 0.287 mmol) and K_3PO_4 (1.22 g, 5.75 mmol) along with **1a** (700 mg, 2.30 mmol) and **1b** (524 mg, 1.9 mmol). The reaction mixture was refluxed for 24 hours. After cooling to room temperature, the solution was filtered through a celite plug and the filtrate was diluted with ethyl acetate, washed with water (3x) followed by brine, and dried over $MgSO_4$, Finally, the solvent was removed under vacuum. The crude product was purified by column chromatography (SiO_2, 1:3 EtOAc:Hex, R_f = 0.52). Purification yielded a yellow solid (525 mg, 80%). ^{1}H NMR (500 MHz, $CDCl_3$) δ 8.89 (bt, J = 1.7 Hz, 1H), 8.55 (s, 1H), 8.33 (d, J = 1.7 Hz, 2H), 8.07 (d, J = 8.5 Hz, 2H), 7.49 (m, 4H), 7.37 (dd, *J* = 7.5, 7.5 Hz, 2H), 3.96 (s, 6H). ^{13}C{^{1}H} NMR (126 MHz, $CDCl_3$) δ 166.34, 139.91, 136.65, 134.41, 131.41, 131.19, 130.21, 130.13, 128.69, 127.64, 126.18, 126.11, 125.38, 52.59.

5-(Anthracen-9-yl)-isophthalic acid (2) was prepared *via* a modification of a previously reported method.[29] Compound **1c** (850 mg, 2.29 mmol), was added to a solution of NaOH (6 M, 15 mL), methanol (15 mL), and degassed THF (15 mL). This solution was refluxed for 23 h. After cooling to room temperature, the solution was concentrated by rotary evaporation and cooled in an ice bath. Cold, concentrated HCl was added until yellow precipitate formed. The precipitate was recovered by filtration, washed with EtOAc and dried under reduced pressure (742 mg, 94%). ^{1}H NMR (500 MHz, DMSO-d_6) δ 13.45 (bs, 2H), 8.76 (s, 1H), 8.69 (t, *J* = 1.6 Hz, 1H), 8.20 (d, *J* = 8.7 Hz, 2H), 8.13 (d, *J* = 1.6 Hz, 2H), 7.56 (m, 2H), 7.7 (m, 4H).

N1,N3-*bis*(6-Pivalamidopyridin-2-yl)-5-(anthracen-9-yl)-isophthalamide (**2a**) was prepared as follows. Compound **2** (100 mg, 0.314 mmol) was placed in a round-bottom flask under inert atmosphere to which 3 mL $SOCl_2$ as added slowly followed by one drop of DMF. This solution was stirred and heated for 2 hours. $SOCl_2$ was then removed under vacuum, and then the crude acid chloride was dissolved in dry THF. Separately, TEA (95 mL, 0.67 mmol) and N,N'-(pyridine-2,6-diyl)dipivalamide (121 mg, 0.579 mmol), which was prepared as previously reported,[21,30] were dissolved in 20 mL dry THF. This solution was cooled to 0 °C and then the acid chloride solution was added dropwise. After addition, a yellow precipitate formed, and the solution was stirred and allowed to warm to room temperature overnight. The yellow precipitate was recovered by filtration, dissolved in EtOAc, filtered through a celite plug and then dried under vacuum. The crude product was purified by column chromatography (SiO_2, 1:2 EtOAc:Hex) and yielded a yellow solid. (32 mg, 15%) ^{1}H NMR (500 MHz, DMSO-d_6) δ 10.64 (s, 2H), 9.96 (s, 2H), 8.77 (d, J = 7.2 Hz, 2H), 8.22 (m, 4H), 7.81 (m, 6H), 7.58 (t, J = 8.6 Hz, 4 H), 7.49 (m, 2H), 2.28 (s, 2H), 1.00 (s, 18H). ^{13}C{^{1}H} NMR (126 MHz, DMSO-d_6) δ 170.88, 164.98, 150.52, 150.06, 139.99, 138.47, 134.71, 134.44, 133.47, 130.85, 129.47, 128.56, 127.27, 127.11, 126.27, 125.90, 125.44, 110,71, 109.99, 40.95, 30.86, 29.55. HMS (ESI-TOF) *m/z*: $[M + H]^+$ Calcd for $C_{44}H_{45}N_6O_4$ 721.3502, found 721.3498.

Reference electrode preparation

Ag/AgCl reference electrodes were made in-house. Ag/AgCl wires were prepared by soaking silver wire (0.5 mm dia) in household bleach for 12 hours. The electrode body was formed by pressing a molecular sieve into the tip of a tapered polypropylene syringe column (Norm-Ject 4010.200v0). One end of each silver wire was then soldered to a 20 AWG tinned copper wire and

the solder joint completely encased in Loctite Marine Epoxy (1919324). Agarose at 2 wt% was dissolved in warm 3 M KCl. 0.8 mL of this solution was poured into the syringe bodies and allowed to cool. The finished electrodes were stored in a 3 M KCl solution overnight before initial use. Reference potentials were found to be 129-146 mV vs SCE.

Membrane and device preparation.

FETs (WIPS-C) with unmodified silicon nitride gates were purchased from Winsense™ (www.winsense.co.th, WIPS-C). These arrive pre-bonded to small printed circuit boards on which the source and drain can be accessed via contact pads. These pads were soldered to 20 AWG tinned copper wire and the solder joints were completely encased in Loctite Marine Epoxy (1919324) leaving only the FET surface exposed. Prior to modification, these were cleaned by soaking in 30% H_2O_2 for 15 minutes, rinsing with deionized water followed by ethanol. NBR (nitrile butadiene rubber) membranes were applied by drop casting (see drop casting solution preparation below) using a 1-5 µL adjustable volume pipette. In general, 10 drops of approximately 1.6 µL were applied to reach a thickness of approximately 100 µm. Drops were applied every 12-15 minutes. After drop casting, sensors were conditioned in an oven at 80 °C for 12-16 hours. After cooling to ambient temperature and then soaking in 0.1 M sodium nitrate solutions for 30-45 minutes, the sensors were ready for use. Initial testing revealed sensors had operational lifetimes of for over 36 hours.

A general method for preparing drop cast solutions for barbituric acid-sensitive membranes follows: Formulation IV incorporates 0.25 wt% tetraoctylammonium nitrate (TOAN) , 5 wt% nitrile butadiene rubber (NBR), and 0.125 wt% receptor **1** which were dissolved in anisole.

Formulation VI is comprised of 25 wt% TOAN, 5 wt% NBR, 0.125 wt% receptor **2a**. Formulation IV contains 5 wt% NBR and 0.25 wt% TOAN.

Potentiometric measurements.

The ChemFETs were driven by an instrumentation amplifier obtained from Winsense^{TM} which maintains a drain voltage (V_{DS}) at 617.5 mV and the drain current (I_D) at 99.6 μA. The circuit holds an external reference electrode at ground while V_{GS}, the voltage between ground and source, is changed to maintain V_{DS} and I_D and is recorded as the measurement signal. An NI-DAQ 6009 data acquisition unit paired with a custom LabVIEW ^{TM} program was used for monitoring and recording measurements. The signal was recorded at a rate of 1 kHz. Unless otherwise noted, each measurement was taken as the average of the signal over the 300th second of the measurement period and experiments were performed with four identical (replicate) sensors and in triplicate.

Potentiometric measurements were performed at ambient temperature in 50 mL polypropylene centrifuge tubes. The solutions were prepared fresh for each experiment by the addition of solid sodium barbiturate into 50 mM PIPES pH 7.0 buffer solution followed by heating of these solutions (50-70 °C) with stirring until dissolved (15-30 minutes). The final stock solutions were light pink in color. The PIPES buffer itself was made by combining solid PIPES with deionized water followed by the dropwise addition 4M KOH until all solid dissolved. The pH was then further adjusted to pH 7.0 using 4M KOH.

Results and Discussion

In previous work, binding constants for 1 and 2b were determined by performing ^{1}H NMR titrations with barbital (R_1=R_2=Et in Figure 2.2), a common barbiturate derivative that exhibits

high solubility and affinity for Hamilton receptors in $CDCl_3$ and is neutral at physiological pH.[21] Binding was observed through the shifting of N-H peaks on both the host and guest molecules. We determined that conventional receptor 2b (Appendix A) has an association constant (K_a) for barbital of 174 M^{-1} and the deconstructed receptor **1** has a corresponding K_a of only 2 M^{-1}. Interactions in these systems were found to occur through complementary ADA-DAD hydrogen bonding of the amide groups of both the host and guest molecules on each side of the guest. The anthracene core of **2a** should not convolute or contribute to the barbiturate binding event as the anthracene core is orthogonal to the binding pocket. However, the additional hydrophobicity, in comparison to **2b**, may help affix the receptor inside the ISM.

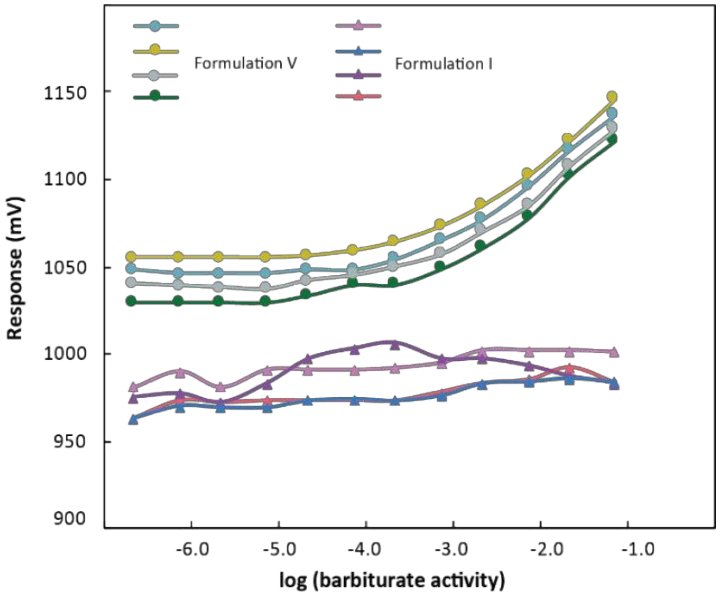

Figure 2.4 Normalized responses of a set of four ChemFETs using Formulation **V** compared to a set using Formulation I.

Sensor construction and calibration

After confirming the binding capabilities of the free receptors, we incorporated **1** and **2a** into ISMs, applied these membranes to ChemFET devices and tested the devices based on the

performance of the ISMs. To begin, membranes were prepared with varying compositions of **1** or **2a**, the lipophilic salt TOAN, and NBR. TOAN was included because when neutral receptors such as **1** and **2a** are used in ISMs, positively charged lipophilic additives are often required for optimal (Nernstian) response. Indeed, devices that were prepared with membranes lacking TOAN showed no response to barbiturate (see Table 2.1 and Figure 2.4).

Once the sensors were prepared, calibrations were performed in order relate the concentration of analyte in a series of sodium barbiturate solutions to observed voltage response. ISMs containing varying quantities of receptor and lipophilic salt were prepared and devices based on these membranes were evaluated (see Table 2.1). We observed the highest sensitivity and lowest detection limit for the following formulation: 0.125 wt% **1** with 0.250 wt% TOAN (Formulation V, Table 2.1). These ratios are similar to ISMs previously reported, in which lipophilic cations are used alongside charge neutral receptors to target anions.[3,30] After optimization, we prepared analogous devices based on an ISM containing **2a** and also devices whose ISMs contained only TOAN. We observed that the TOAN-only devices exhibit sensitivity although this sensitivity is significantly reduced compared to devices whose ISMs included receptor **1** or **2a**. ISMs containing Formulation **V** show statistically higher sensitivity at 50 mV/dec compared to the TOAN-only ISMs (Formulation **IV**, Table 2.1).

Additionally, this formulation exhibits higher selectivity for the majority of interferents tested. Taken together, these results indicate that the Hamilton-type receptors contribute to the anion selectivity and sensitivity of the devices.

Table 2.1 Optimization of the ion-selective membranes using receptors shown in Figure 2.2a.

Formulation	Composition	Sensitivity (mV/dec)	LOD (mM)
I	0.125 wt% **1**	NR*	NR*
II	0.125 wt% TOAN	35±2	6±2
III	0.125 wt% **1** + 0.125 wt% TOAN	24±1	0. 51±0.09
IV	0.250 wt% TOAN	44±3	10±3
V	0.125 wt% **1** + 0.250 wt% TOAN	50±1	0.64±0.07
VI	0.125 wt% **2a** + 0.250 wt% TOAN	48±2	5.1±0.7

*Sensitivities and detection limits are an average of 4 sensors recorded in triplicate

Selectivity evaluation

The practicality of chemical sensors is largely dependent on the selectivity of the sensors for their target analyte. Selectivity is a crucial figure of merit for such sensors and is governed by the composition of the ISM. Selectivity coefficients describe the ability of a device to distinguish between its analytical target and a potentially interfering species. We determined selectivity coefficients using the Fixed Interference (FI) method. Briefly, this technique involves measuring the response of sensors in the presence of constant interferent activity. A selectivity coefficient, $K_{A,B}^{pot}$ can be calculated with the following equation:

$$K_{A,B}^{pot} = \frac{a_A}{a_B^{z_A/z_B}}$$

where a_A is the extrapolated LOD and $a_B^{z_A/z_B}$ is the activity of the interferent at the LOD. A value of less than 1 indicates the sensor is selective for the target over the interferent.[32] Interferents Cl^-,

HSO_4^-, $H_2PO_4^-$ and HCO_3^- were selected based on potential presence in environments where barbiturate can be found. Sodium urate was examined due to the similar ADA hydrogen bonding (HB) motif.

Results of selectivity studies performed with sensors containing **1**, **2a**, and as well as sensors containing only TOAN are summarized in Table 2.2.[32] $K_{A,B}^{pot}$ values are shown in Figure 2.5. All ISM formulations show considerable selectivity over Cl^-, HSO_4^-, $H_2PO_4^-$, and HCO_3^-. Of these, chloride demonstrates the highest interference with barbiturate detection. Notably, there was minimal interference from $H_2PO_4^-$ even at concentrations of 1.0 M. We observed high interference from urate, presumably due to it possessing a hydrogen bonding ADA motif like that of barbiturate. The addition of interferent had minor diminishing effects on the BBA sensitivity of sensors containing no receptor whereas the ISM with **2a**, experienced a noticeable drop in response across all interferents (Table 2.2).

Table 2.2. Sensitivity responses for the given selectivity studies.

Interferent	IV(mV/dec)	V(mV/dec)	VI (mV/dec)
None	44±3	50±1	48±2
100 mM Cl^-	37±1	44±1	23±1
200 mM HSO_4^-	44±2	52±1	29±1
150 mM HCO_3^-	37±1	47±2	31±1
1.0 M HPO_4^-	39±2	45±2	34±2
0.5 mM $C_5H_3N_4O_3^-$	37±2	44±2	26±1

*IV contains no receptor, V includes receptor 1 and VI contains receptor 2b. Sensitivities are an average of 4 sensors recorded in triplicate.

Alternative testing matrices

To demonstrate the practicality of these devices, we selected different aqueous matrices, including neutral PIPES buffer, neutral buffer containing xanthine, Willamette River (Oregon) water, and synthetic urine (see Figure 2.5 for structures). ChemFETs with formulation V (Table 1) were prepared and tested in barbiturate-spiked samples of the matrices.

Figure 2.5 Sodium barbiturate and potential interferents having similar "ADA" structural motifs.

Under these conditions, the sensors exhibit near-Nernstian sensitivity for barbiturate in river water and synthetic urine (Table 2.3). Xanthine, a purine base found in tissue with a similar HB motif as barbituric acid, had little effect on sensitivity but did induce a slightly higher LOD than the other systems studied. Overall, these tests illustrate the rugged performance of the barbiturate sensitive ChemFETs.

Table 2.3 Sensitivity responses in various aqueous matrices.

Analyte Matrix	Sensitivity (mV/dec)	LOD (mM)
PIPES buffer (pH 7.0)	50±1	0.64±0.1
Synthetic urine	56±2	0.63±0.1
River water	60±1	0.65±0.1
5 mM xanthine in buffer	49±2	2.9±0.4

Results are an average of 4 sensors tested in triplicate.

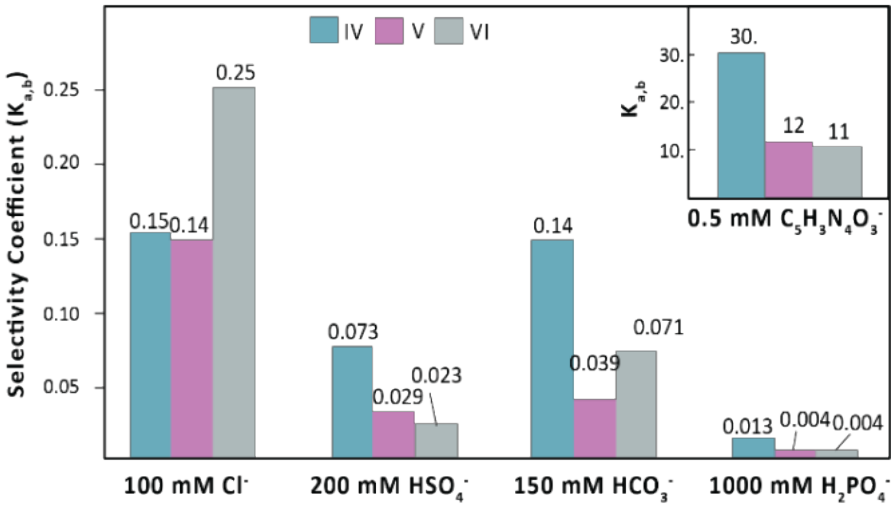

Figure 2.6 Selectivity coefficients determined using the fixed interferent method.

Conclusions

In summary, Hamilton receptors **1** and **2a** exhibit strong binding to barbiturate derivatives in solution studies. Upon incorporation into polymer-based ISMs and applying those membranes to ChemFETs, both receptors enhanced device barbiturate sensitivity and selectivity. In addition, the sensors exhibited moderate sensitivity and selectivity for barbiturates even in the presence of interferents.

Additionally, the robustness of the sensors was demonstrated by investigating various aqueous matrices where near-Nernstian sensitivity and detection limits below 1 mM were observed. Additionally, we demonstrated that unlike in solution, the receptor preorganization has no effect on the sensitivity or selectivity when in an ISM material. This difference is evident when comparing the selectivity coefficients of the different ISMs (Figure 2.6). These results are contrary to the trend observed in solution studies, which revealed that more preorganized Hamilton receptors exhibit stronger affinities for the target analyte. Moving forward, comparisons should

continue to be made between free and membrane-bound receptor binding capabilities to better inform receptor design for both media.

Bridge to Chapter III

The research presented in Chapter II is a clear example of how electrical sensors can be used to target negatively charged small molecules using a polymer membrane with a synthetic host. In Chapter II, the selectivity is influenced by the inclusion of a Hamilton-type receptors- a synthetic motif known to have a complementary hydrogen bonding structure to the barbiturate conjugate base. The results show a preference for barbituric acid over inorganic anions but also displayed selectivity for similar structures, such as urate. In Chapter III, focus will shift to hydrosulfide (HS-). The conjugate base of recently discovered gasotransmitter hydrogen sulfide, is a challenging sensing target due to the anion's oxidizing nature. In the following Chapters (III and IV), HS- is investigated using two different bases for a polymer-coated ChemFET. This work has potential impact to industrial safety, biological monitoring, and environmental remediation practices.

CHAPTER III

HYDROSULFIDE-SELECTIVE CHEMFETS FOR AQUEOUS H_2S/HS^- MEASUREMENT

This chapter was previously published as "Sherbow, T. J., Kuhl, G. M., Lindquist, G. A., Levine, J. D., Pluth, M. D., Johnson, D. W., & Fontenot, S. A. Hydrosulfide-selective ChemFETs for aqueous H_2S/HS^- measurement. *Sensing and Bio-Sensing Research* **2021,** *31*, 100394."

Introduction

Hydrogen sulfide (H_2S) is an important analytical target for a diverse set of sensing applications including environmental sensing, biomedical sciences, and petroleum and natural gas industries. H_2S is produced during the decomposition of organic matter and is naturally present in ponds, swamps, and in landfills and sewage systems. H_2S is also found in natural gas and crude oil and is considered a contaminant in refined petroleum and gas products.[1] Due to the toxicity and environmental prevalence of H_2S (from both natural and unnatural sources) further development of environmental H_2S sensing methods is needed.[2] H_2S has also been established as an important small molecule biological mediator and is associated with different physiological conditions including diabetes, hypertension, neurodegeneration, and heart failure.[3-8]

Thus far, there are critical disadvantages to current aqueous H_2S measurement methods that limit their utility in different sensing environments. Reaction-based analytical methods, such as monobromobimane (mBB) sulfide trapping, feature excellent detection limits (below 200 nM)

yet these methods require long reaction/measurement times and extensive sample preparation.[9-11] Alternatively, amperometric H_2S measurement methods exist and devices that support these are available, with primary suppliers being Unisense (Aarhus, Denmark) and World Precision Instruments (Sarasota FL, USA). These also offer excellent detection limits (5-100 nM), however, they have comparatively short lifetimes, can suffer from interference from common sulfide species such as cysteine, glutathione, sulfur dioxide, dimethyl sulfoxide, and alkyl thiols, and require highly sensitive electronics to resolve very small signal currents, which can be as low as 10^{-13} Amperes. For many environmental samples, gas chromatography (GC) methods are adequate, but such methods are less convenient and much more resource intensive than sensor-based methods.[12, 13] Overall, there are opportunities to develop new technologies and methods for measuring H_2S in a variety of physiologically and environmentally relevant applications and sample matrices. The diversity of sensing environments and associated detection ranges necessitate new chemical tools for H_2S detection and measurement. Potentiometric methods in particular have been poorly represented in environmental, petrochemical, and biological application spaces.[12]

H_2S has a pK_a near 7 and is largely present as its conjugate base, hydrosulfide (HS^-), at physiological temperature and pH.[13] As an ion, HS^- is susceptible to direct detection by potentiometric methods, which are rarely considered for aqueous H_2S/HS^- measurement.[14] Herein, we present a new method for direct measurement of aqueous HS^- using chemically sensitive field effect transistors (ChemFETs). Examples of ChemFETs, OFETs, and other FET-based sensors for hydrogen sulfide exist for the gas phase;[15-18] yet there are not, to our knowledge, any examples of potentiometric methods, FET-based or otherwise, for direct measurement of the hydrosulfide anion in water.

ChemFETs are often described as metal-oxide-semiconductor field effect transistors (MOSFETs), which have had the gate electrode separated from the gate oxide and the now-exposed gate oxide modified to be selective for specific chemical species.[19] Often this modification involves the application of a chemically selective membrane to the gate oxide. Some benefits of ChemFETs include their quick response times, minimal sample processing requirements, and a library of well-established methods for manipulation of their surface chemistries and for modification of the gate oxide interface with chemical recognition agents.[20-22]

The ChemFETs described in this work feature a polymer membrane formulated with a non-covalently associated HS^- ionophore, and they provide detection of HS^- in real-time with selectivity over sulfur-containing compounds including cysteine and glutathione, which are common interferants in H_2S measurements. These devices enable measurement methods which require minimal sample preparation (simple pH adjustment) to ensure that HS^- is present and that H_2S is not lost due to degassing from the solution that is being measured.

ChemFET overview

ChemFETs function according to similar principles as MOSFETs. In short, the threshold voltage of an enhancement mode ChemFET (V_{th}^{CFET}) is related to the activity of chemical species present in solution between the gate electrode (which may be a reference or pseudo-reference electrode) and the gate oxide. V_{th}^{CFET} is defined as the minimum potential between the ChemFET gate electrode and source required to open the conducting channel between the source and drain. V_{th}^{CFET} itself is the sum of threshold voltage of the underlying FET (V_{th}^{FET}) and the combined contributions from the rest of the chemical cell, V_{cell}.

$$V_{th}^{CFET} = V_{th}^{FET} + V_{cell} \tag{3.1}$$

V_{th}^{FET} is determined by the materials and geometry of the FET portion of the device and is independent of most environmental variables. Therefore, V_{th}^{FET} is effectively constant, and a change in V_{th}^{CFET} is the result only of a corresponding change in V_{cell}.

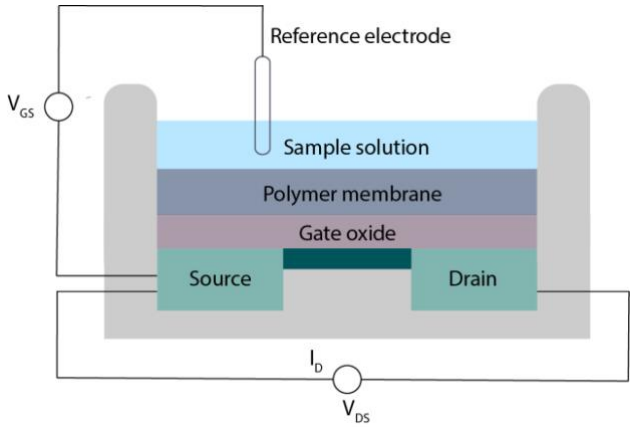

Figure 3.1 Schematic illustration of a ChemFET featuring the polymer membrane at the interface between the sample solution and the gate oxide. The operational mode of the ChemFET is such that $V_{th}^{CFET} = V_{GS}$, which is taken as the measurement signal.

Physically, the cell includes the environment between the gate oxide, the chemically selective material, the sample environment, and the reference electrode (Figure 3.1). This environment includes several chemical and material interfaces each with an associated junction potential. Fortunately, not all of these potentials need to be considered or even known. When ideally constructed, the junction potential of the chemically selective material is the only variable and therefore a change in V_{cell} and the corresponding change in V_{th}^{CFET} is due solely to the activity of the target ion. This requires, at minimum, a reference electrode that is insensitive to changes in

target ion concentration and a chemically selective material that responds primarily to the desired analytical target.

In practice perfect selectivity is elusive and the relationship between V_{cell}, the activities of the analytical target (A), and the activity of a potential interferent (B) can be described by the Nikolsky-Eisenmann equation.[20, 23]

$$3.2 \qquad V_{cell} = V_{cons} + \frac{2.303\,RT}{z_A F} log\,(a_A + K_{A,B}\,a_B^{z_A/z_B}) \qquad (3.2)$$

V_{cons} represents the sum of all the constant interfacial potentials in the cell, a_A and a_B are the activities of A and B, and z_A and z_B are the corresponding ionic charges of A and B. *R* and *F* are the ideal gas constant and Faraday constant, respectively, and *T* is temperature. Finally, $K_{A,B}$ is the experimentally determined selectivity coefficient representing the ability of the ChemFET to distinguish between A and B. Since the only variables affecting V_{cell} are a_A and a_B, ΔV_{th}^{CFET} depends entirely on ΔV_{cell} (again, V_{th}^{FET} is constant). What remains then is to transduce V_{th}^{CFET} into the measurement signal.

Note that in the absence of an interfering ion, a_B, equation 2 reduces to a form of the Nernst equation which, when *T* is 25 °C and when z_A, is +1 or -1, is

$$3.3 \qquad V_{cell} = 0.059\,V\,log_{10}\,a_A \qquad (3.3)$$

According to Equation 3, 59 mV represents the maximum possible change in V_{cell} for each decade change in the activity of an ionic species having a charge of +1 or -1. This is referred to as the Nernstian limit.

Experimental

Reagents and solutions

Sodium hydrosulfide (NaSH) was purchased from Strem Chemicals and stored in a nitrogen filled glovebox. All other reagents and solvents were purchased from Sigma-Aldrich or Tokyo Chemical Industry (TCI) and used as received. Note that NaSH and ammonium sulfide are toxic and will liberate H_2S when exposed to water. All handling of these chemicals should be performed in a glove box or fume hood to prevent personal exposure and a zinc acetate quench solution should be available at all times.[24,25] Additionally, a personal H_2S meter should be used monitor exposure to H_2S.

Membrane and sensor preparation

Nitrile butadiene rubber (NBR) was obtained from Zeon Chemicals (Nipol DN401LL). FETs with unmodified gate oxides were purchased from Winsense™ (www.winsense.co.th, WIPS-C). These pre-functionalized FETs were cleaned immediately prior to modification by soaking in 30% H_2O_2 for 20 minutes followed by rinsing with DI water and then with ethanol. Chemically selective membranes of approximately 150 µm thickness were applied to the gate oxide by drop casting. Sulfide-sensitive membranes were made as follows: 0.1 wt% Tetraoctylammonium (TOA) nitrate and 5 wt% NBR were dissolved in anisole. These solutions were drop cast onto the gate oxide surface and then dried at ambient temperature for 15 min

followed by 80 °C for 12 h. After cooling to ambient temperature and then soaking in 1 M sodium nitrate solutions for approximately one hour, the sensors were ready for use.

Reference electrode fabrication.

Ag/Ag_2S reference electrodes were made as follows: Ag/Ag_2S wires were prepared by soaking silver wire (99.9%, 0.5 mm dia) in 5% ammonium sulfide solution overnight. One end of each wire was then soldered to a 20 AWG tinned copper wire and the solder joint completely encased in Loctite Marine Epoxy (1919324). To form each electrode body, a 4Å molecular sieve was pressed into the tapered end of a 1 mL polypropylene syringe body (Norm-Ject 4010.200v0). Agarose at 2 wt% was dissolved in warm 3 M KCl. 0.8 mL of this solution was poured into the syringe bodies and allowed to cool. Then the Ag/Ag_2S wire was inserted into the electrode body and the wire secured to the housing. Reference electrodes were stored in 3 M KCl overnight before their first use. Reference potentials were found to be 129-146 mV vs SCE.

Electrode surface characterization

Elemental composition and surface morphology were determined by scanning electron microscopy energy dispersive X-ray spectroscopy (SEM-EDS) using a ThermoFisher Helios Hydra Plasma FIB. Images were collected with an accelerating voltage of 10 kV. Additional elemental analysis was performed using Thermo Scientific ESCALAB 250 X-ray photoelectron spectrometry (XPS) system with an Al Kα monochromated source at 20 kV. Survey spectra were taken along with high-resolution scans of Ag 3d, S 2p, and Cl 2p. Spectra were peak fit using the Thermo Scientific Avantage 4.88 software to determine surface composition.

Results and Discussion

Reference electrode fabrication and Characterization

ChemFETs can be used alongside conventional Ag/AgCl reference electrodes, however, due to the corrosive properties of aqueous sodium hydrosulfide, an alternative reference electrode (RE) is required for potentiometric measurements in the presence of hydrosulfide. Initially, Ag/AgCl REs were used for evaluating ChemFET performance, however, we observed inconsistent RE function and drift during measurements and hypothesized that the chloride on the Ag wire surface reacts with sulfide species. This undesired reactivity at the electrode would change the junction potential of the RE which would manifest as signal drift.

To test this hypothesis, four samples of Ag wire were exposed to different treatments: two were submerged in household bleach (sample **1** and **3**) or 5% ammonium sulfide (sample **2** and **4**) for 2 hours. Electrodes **3** and **4** were soaked in a pH 8 NaSH solution for 8 hours after being soaked in bleach and ammonium sulfide, respectively.

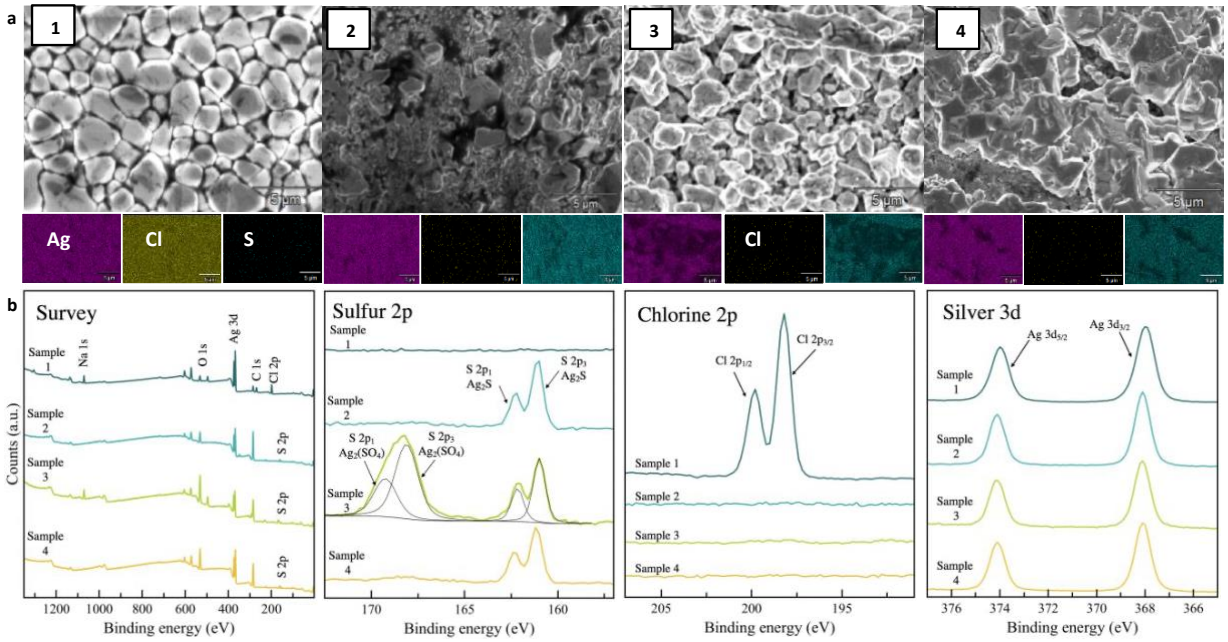

Figure 3.2 a) SEM-EDS images of Ag wire samples 1–4. 1) Control. Ag/AgCl. 2) ammonium sulfide. 3) Ag/AgCl and then NaSH. 4) Ammonium sulfide and then NaSH. b) XPS spectra of elements of interest (Cl, S, Ag) in samples 1 (blue), 2 (aqua), 3 (green) and 4 (yellow). (For interpretation of the references to colour in this figure legend, the reader is referred to the web version of this article.)

The four electrode wires were then analyzed by scanning electron microscopy coupled with electron dispersive X-ray spectroscopy (SEM-EDS) to compare the morphology and elemental composition before and after exposure to NaSH solutions. X-ray photoelectron spectroscopy (XPS) was used to confirm composition. SEM-EDS imaging (Figure 3.2b) displays the morphology of each sample as well as elemental maps of the silver, chlorine, and sulfur. The elemental composition given by XPS is confirmed, and the atomic percentages (Table S1) from sample **3** closely match that of samples **2** and **4** which would be expected to only have sulfur on

the surface of the wire. Figure 3.2a displays the XPS survey spectra and high-resolution scans of samples **1**, **2**, **3** and **4**. Survey spectra indicate that Ag, Cl and Na are the main elements present in sample **1** and Ag and S the main elements in samples **2**, **3** and **4**. All four samples show the presence of C and O from adventitious hydrocarbon present in the XPS instrument. The peaks at 368.1 eV and 374.1 eV can be assigned to the binding energy of Ag $3d^{3/2}$ and Ag $3d^{5/2}$ present from the Ag^{+} in AgCl (sample 1) and Ag_2S (sample 2/3/4). High resolution scans of Cl 2p shows the presence of Cl in sample **1** and relatively small amount (0.4%) present in sample **3**, and none in samples **2** and **4**. Comparison of sulfur spectra presents a significant difference between samples **2** and **3**. The S 2p scan indicates the presence of Ag_2S in samples **2** and **3** at 161 eV and 162.2 eV. However, sample **3** contains peaks at 168.2 eV and 169.2 eV, revealing the presence of $Ag_2(SO_4)$ in addition to Ag_2S. Taken together, this alternative sulfur speciation on the surface of the wire may explain loss in Ag/AgCl reference electrode functionality upon NaSH solution exposure. Critically, samples **2** and **4** are identical, indicating that the Ag_2S surface is stable to the NaSH-containing solutions in which the potentiometric measurements were to be made. These data provided suggested that the Ag/AgCl would not be useable for our potentiometric measurements for HS^{-}, prompting us to develop an Ag_2S coated electrode which was more stable to HS^{-} solutions and served as a reference with higher function and more robust.

Potentiometric measurements

The ChemFETs were operated by a circuit which uses an instrumentation amplifier to drive the source to drain voltage (V_{DS}) of the FET at 617.5 mV and the drain current (I_D) at 99.6 μA. The circuit keeps the external reference electrode at ground while the voltage between source and

ground (V_{GS}) is changed in order to maintain V_{DS} and I_D as identified above. V_{GS} is taken as the measurement signal. See Appendix B for a description of the analog circuit.

The analog V_{GS} signal was recorded using a National Instruments DAQ 6009 data acquisition unit connected to a Windows™ computer and operated by a custom LabView™ program. The signal was recorded at a rate of 1 kHz. Unless otherwise noted, each measurement was taken as the average of the signal over the 120th second of the measurement period and experiments were performed with four identical (replicate) sensors and in triplicate. All sensors were paired with Ag/Ag_2S reference electrodes.

HS^- solutions were prepared in an oxygen-free glovebox or using Schlenk techniques to prevent oxidation. Potentiometric measurements were carried out at ambient temperature in 50 mL polypropylene centrifuge tubes which were kept sealed for the duration of the experiment in order to minimize loss of (and human exposure to) sulfide. The solutions were prepared by the addition of solid NaSH to a degassed 50 mM PIPES pH 8.0 buffer solution. The PIPES solution itself was prepared by dissolving 1,4-Piperazinediethanesulfonic acid in DI water and adjustment of the pH with analytically pure 4 M KOH. This alkaline solution was chosen to limit the protonation of HS^- which accelerates loss of H_2S from the calibration solutions. Activity coefficients were calculated using the Davies equation. Selectivity coefficients were determined by the Fixed Interference method according to IUPAC recommendations.[29] All uncertainties are reported as Standard Error of the Mean (SEM).

Discussion

The key feature of our HS^- selective ChemFETs is the application of a polymer membrane that includes the CRE to the silicon nitride gate oxides of commercially available pH-sensitive

ISFETs. ChemFETs have been reported having chemically selective membranes comprised of PVC, PDMS, and occasionally NBR among other formulations.[22,26-29] Generally, the polymers themselves have limited native sensitivity to ionic targets and their sensitivity/selectivity is be imparted by incorporating chemical recognition elements (CRE) into the polymer membranes to create the interfacial chemically selective material of the device.

Tetraoctylammonium was chosen as our CRE. Quaternary ammonium salts are perhaps most studied for anion sensing applications because they are stable cations and many are lipophilic enough to remain in the polymer membranes without covalent attachment. TOA and other quaternary ammonium salts have been incorporated into ChemFETs, ion selective electrodes, and other potentiometric sensing platforms; some of which have been shown to be functional for up to eight weeks in aqueous environments.[30] Also, quaternary alkyl ammonium salts of HS^- have been shown to associate with HS^- in particular via weak C-H hydrogen bonding interactions, suggesting that this ionophore might serve as a recognition agent for HS^- in its own right.[31]

NBR was chosen as the polymer component of the membrane primarily because NBR membranes enable the tetraoctylammonium CRE to be incorporated into the material without the requirement of any plasticizers or other fillers or additives. NBR has also proven inert to the sample conditions and adheres to the gate oxide well enough to allow an operational lifetime of over 46 hours.

Sensitivity and calibration

To obtain a measurement signal from a ChemFET, an analog circuit must be used to interface with the FET and reference electrode.[32] Hydrosulfide-selective sensors were operated in a constant current configuration in which the input voltage (V_{DS}) and drain current (I_D) are

maintained in a feedback mode such that the gate voltage (V_{GS}), which is the potential between the reference electrode and source, is equal to the threshold voltage of the ChemFET (V_{th}^{CFET}). V_{GS} is then taken as the measurement signal. For this system V_{GS} is in the range of 0.5-3 V which may be accurately measured using comparatively simple equipment such as a basic multimeter or a simple data acquisition device such as a National Instruments DAQ 6009 (See Appendix B).

Potential response curves of devices functionalized with NBR and TOA are shown in Figure 3.3. When TOA was not included in the NBR membrane, no hydrosulfide response was observed. Devices with membranes containing NBR and TOA have near-Nernstian sensitivities of 53 ± 2 mV per decade from 20 to 450 mM and a detection limit of 7.7 ± 0.6 mM. These results suggest that TOA is a necessary chemical recognition agent in these devices.

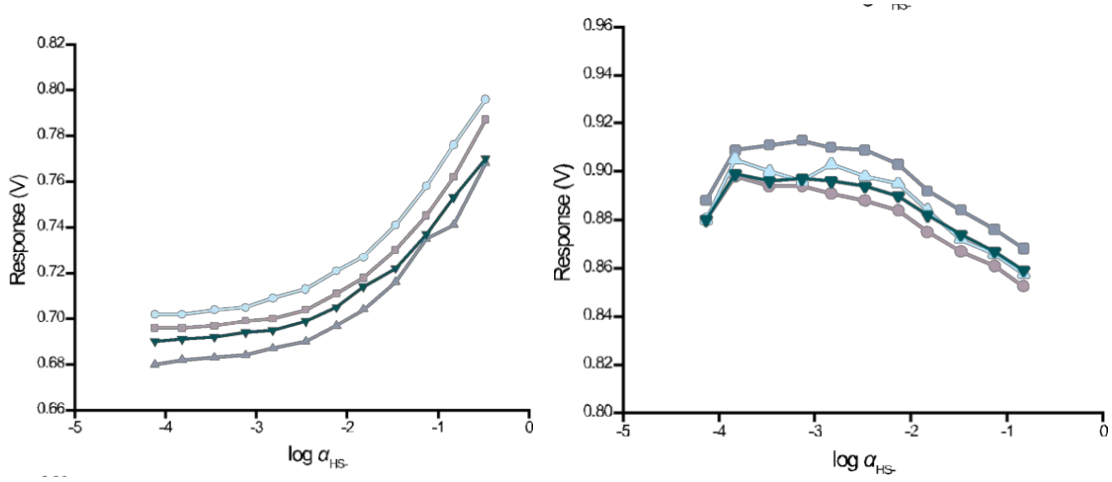

Figure 3.3 (Left) Calibration runs of four identical sensors functionalized with TOA/NBR membrane showing a linear response to hydrosulfide activity (a_{HS^-}) in 50 mM PIPES buffer from approximately 10 to 450 mM HS^-. (Right) The responses of four identical sensors are shown.

Response time and reversibility

Sensor responses were recorded continuously for 300 s. As shown in Figure 3.4, the devices reach their equilibrium responses (having a drift of less than 1 mV per min) within 120 s except for very high concentrations (450 mM) in which the drift was as high as 5 mV per min.

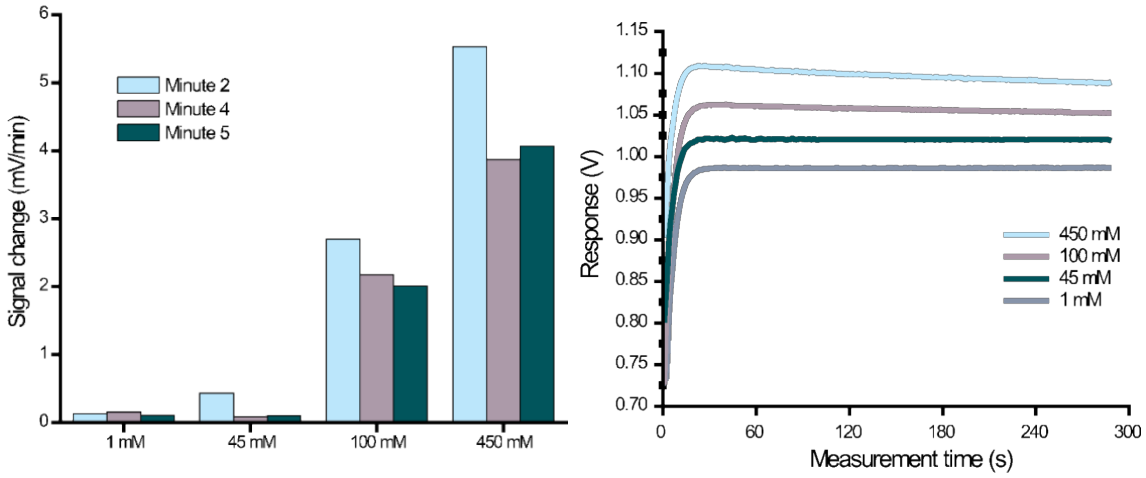

Figure 3.4 (Left) Signal drift calculated for four different HS^- concentrations from 60 to 120 s (Minute 2), 180–240 s (Minute 4) and 240–300 s (Minute 5). (Right) Measurement signals recorded from the time the sensor was powered on.

As a compromise between efficiency and accuracy and to limit the exposure of the FETs and reference electrodes to high concentrations of sulfide, measurement responses were generally taken as the potential of V_{GS} at 120 s. The reproducibility of three calibration experiments is shown for a single sensor by measuring varying [HS^-] in pH 8 PIPES buffer (Figure 3.5). The first and last experiments were performed in order of descending hydrosulfide concentration while the

second experiment was run in the reverse direction, showing negligible hysteresis and that the single sensor maintains repeatable HS^- response characteristics.

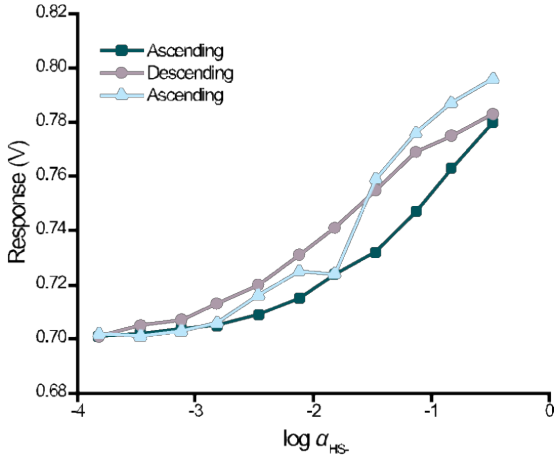

Figure 3.5 Reproducibility of three consecutive calibration experiments for hydrosulfide at pH 8 in the 50 mM PIPES buffer.

Selectivity Studies

The practicality of chemical sensors depends largely on their selectivity for their target over other chemical species. The Fixed Interference method was used to determine selectivity coefficients for hydrosulfide ($K_{SH,X}$) over thiol-containing small molecules such as glutathione (GSH) and cysteine as well as chloride.[33] As expected, when significant interference is observed, there is a corresponding increase in the effective detection limit (EDL). In Table 3.1, EDL represents an effective detection limit of these devices for HS^- in the presence of 200 mM of each interferent. These sensors show a favorable selectivity coefficient of 0.12 for hydrosulfide over chloride. Interestingly, the few supramolecular hosts that are able to bind HS^- often show similar binding constants for HS^- and Cl^-, presumably because both ions are of similar size, while our

sensors show almost an order of magnitude preference for HS^- over Cl^-.[34,35] The interfering ability of cysteine is similar to that of Cl^-.

Table 3.1. Summary of selectivity studies performed with TOA/NBR ChemFETs showing selectivity coefficients, effective detection limits, and corresponding standard error.

Interferent (*X*)	**Selectivity Coefficient ($K_{SH,X}$)**	**EDL (mM)**
Chloride	0.12 ±0.02	22 ±2
L-Cysteine	0.13 ±0.04	20 ±8
GSH	0.070 ±0.01	11 ±2

*All interferents were present at a background level of 200 mM. GSH=glutathione.

Conclusions

We report a new FET-based sensing platform effective in measuring hydrosulfide in the presence of other sulfur-containing species. To our knowledge, this is the first reported potentiometric method for direct hydrosulfide detection in water. The sensor is comprised of a commercially available pH-sensitive ISFET which was coated with a polymer membrane containing tetraoctylammonium nitrate. In optimized conditions, sensitivity and detection limit were found to be 53 mV per decade and 8 mM, respectively. The sensor shows a reversible response, and devices retain useful sensitivity for at least 46 operational hours. We are working on further device optimization to access the low detection limits (below 1 μM) required to study HS^- at physiological concentrations. These first-generation ChemFET devices provide a promising lead in this direction with their strong HS^- selectivity, reversible and repeatable sensing, fast response times, and selectivity over common thiol-containing interferents.

Bridge to Chapter VI

The material presented in Chapter III provides context and motivation for Chapter IV by providing an example of a polymer membrane used in conjunction with a potentiometric sensor to detect HS^- in water. Chapter III provides important experimental information with the investigation into Ag/Ag_2S reference electrodes that will be applied in the next work. Additionally, the material above introduces a chemical sensor with modest sensitivity and selectivity, leaving room for improvement. This leads the search for an ionophore to target aqueous HS^-.

CHAPTER IV

INTEGRATION OF DODECABUTYL BAMBUS[6]URIL INTO CHEMFET FOR AQUEOUS ION DETECTION

This chapter contains unpublished experiments performed by Major Douglas Banning, Madeline Howell, and myself. I am the sole author of this chapter with editing assistance from Major Banning.

Introduction

Hydrosulfide (HS^-) is the conjugate base of gasotransmitter hydrogen sulfide, a physiologically-relevant species of great interest in the anion sensing community.[1,2] However, selective sensing of HS^- in water remains difficult because in addition to the diffuse charge and high solvation energy of anions,[3] HS^- is highly nucleophilic and readily oxidizes into other reactive sulfur species.[4] Methods such as monobromobimane[5] and coumarin[6] fluorescence analyses provide high sensitivity; however, these sensors require extensive synthesis, sample preparation, and data analysis that encumber their utility.[4] Supramolecular host-guest chemistry has aided in the design of hydrosulfide-specific receptors for spectroscopic binding studies[1, 2, 6-8] but do not facilitate *in vivo* or *in vitro* studies. Therefore, work must continue towards a simple and fast HS^- detection.

Electrochemical sensors are an option alternative for hydrosulfide detection by offering parallel data collection and are often suitable for portable detection methods.[9] Potentiometric sensors are an inexpensive option with simple instrumentation and sensor can integrated with chip-based devices.[10, 11] This makes them particularly attractive for market applications.[12] Ion selective electrodes impart selectivity with materials including inorganic crystal lattices,[13] lipophilic salts,[14] and metal-ligand coordination[15] to gain selectivity.[16] Membranes containing a lipophilic ion exchanger are a viable option as the polymer and plasticizer properties are well known and easy to process.[17] These will be the feature of this dissertation.

The selective component of these membranes are ionophores which are biological or synthetic structures with tailored noncovalent intermolecular interactions, such as hydrogen bonding and hydrophobic forces.[18] Unfortunately, ISEs suffer from instability related to the inner electrolyte and drift,[19, 20] leaving room for alternate device.

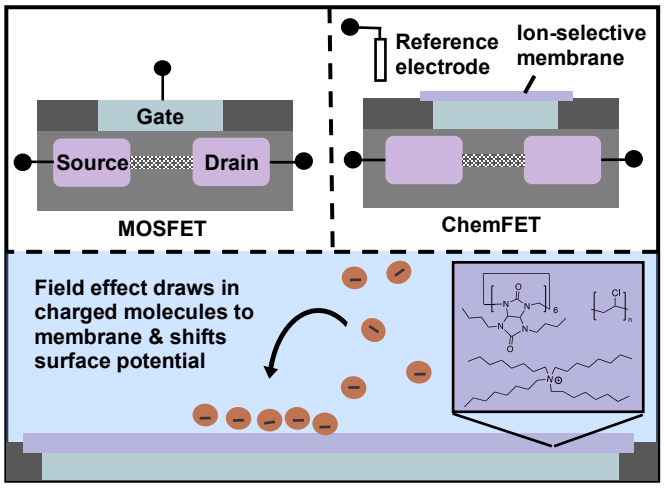

Figure 4.1 A simplified representation of a metal-oxide semiconductor FET (top left) compared to a ChemFET (top right). A cartoon depiction of the field effect and the chemical structures of the membrane components (bottom).

ChemFET response

Chemically sensitive field effect transistors (ChemFETs) are a potentiometric platform employed for ion sensing in water due to their fast response, stability and reusability.[11, 18] ChemFETs have high signal-to-noise ratios, and low sample volume requirements.[20] The ChemFET response is reliant upon the change in potential at the sensing gate, which is covered by an ionophore-doped polymeric membrane (Figure 4.1). Therefore, the response at the membrane/solution interface is described, like an ISE, using the Nikolsky-Eismann equation[14, 18] (Equation 1.2):

$$V_{cell} = V_{cons} + \frac{2.303\,RT}{z_A F}\, log\,(\, a_A + K_{A,B}\, a_B^{z_A/z_B})$$

Where V_{cons} is the sum of all constant potentials within the cell with a total potential V_{cell}. Activities of ions A, B are a_A and a_B, $z_A$and z_B are the respective ion charges. R is the ideal gas constant, T is temperature in °C, and F is Faraday's constant. $K_{A,B}$ is a selectivity coefficient experimentally determined through the fixed interference or separate solutions method.

Although ChemFETs share a logarithmic response to changing concentration like ISEs, they have different internal Briefly, the shifting surface potential impacts a depletion layer between the source and drain terminals.[21] This layer allows electrons to flow and a

current to be measured, and the magnitude is altered by the field effect and directly relates to the concentration of target analyte in the sample solution.[22] For further explanation, see Chapter I, pages 3-4.

Ionophore for the hydrosulfide anion

Recent work introduced the first HS^- ChemFET sensor using a nitrile butadiene rubber (NBR) coating and tetraoctylammonium nitrate as an ionic site additive. [14] This yielded modest selectivity, but also resulted in a method design for HS^- in buffered water. To improve upon the figures of merit from the previously mentioned work, a neutral ionophore in a polymer membrane, which will be discussed further below. We believe a selectivity for hydrosulfide in water can be achieved through embedding a supramolecular ionophore within the polymer membrane of a potentiometric sensor.

Looking to the literature, there are a few options for hydrosulfide binding.[1, 7, 23] In 2018, the Sindelar group reported binding of dodecamethyl bambus[6]uril and dodecanbenzyl bambus[6]uril with HS^- and S^{2-} in buffered water.[8] This is the first known example of a synthetic receptor capable of aqueous hydrosulfide complexation and seemed like a promising option for an ionophore. Bambus[6]urils are a class of supramolecular receptor with 4 or 6 repeating bicyclic glycoluril units connected by a bridging methylene.[24] These receptors are known for their defined cavity size, tunable functional groups, and strong anion affinity in both water and organic solvent.[25-27]

We hypothesize that integrating a bambus[6]uril receptor shown to bind with aqueous HS^- into a ChemFET polymer membrane will increase sensitivity and selectivity towards this anion based on its in-solution binding affinity. To further support this idea,

recent work reported a bambus[6]uril employed as the ionophore in a perchlorate-selective sensor.[28] In addition to measuring sensor device performance towards hydrosulfide, we begin an investigation of the Hofmeister series with the ChemFET.

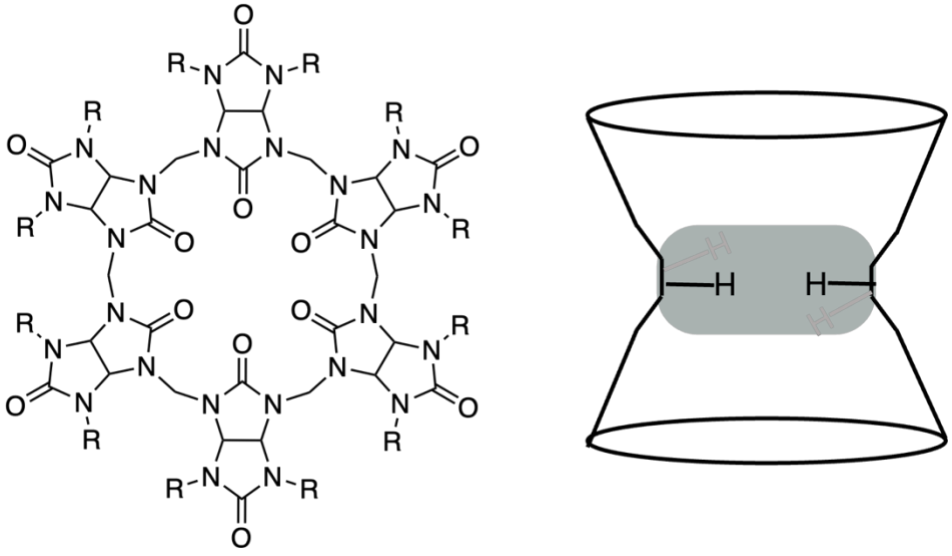

Figure 4.2 (Left) Chemical structure of a bambus[6]uril macrocycle. (Right) Cartoon approximation of the bambus[6]uril geometric structure. The portion highlighted in blue represents where the 12 hydrogens face inward, creating a binding pocket. Note that 8 H's are removed for clarity.

The Hofmeister series

Originally discovered while studying salt effects on protein solubility, the Hofmeister effect is an active area of interest in interfacial and host-guest chemistry.[29, 30] Briefly, ions are ranked based on how stabilizing their presence is to a macromolecule in solution. Anions on the left side (perchlorate, thiocyanate) of the series below increase solubility and decrease surface potential whereas the right hand side increases surface tension and potential while lowering solubility.[31, 32] Although often studied in bulk solution, the effect arises at aqueous interfaces[32] similar to that of an ISE or ChemFET membrane in

an electrolyte solution.[29] The mechanism of the Hofmeister effect is not fully understood but is thought to be attributed to a combination of ion size, hydration energy, polarization, electrostatics, and ion partitioning. In potentiometry, the Hofmeister effect is displayed in the absence of a membrane-bound ionophore. This leads to a characteristic response pattern (i.e., all things being equal, the Hofmeister effect suggests a greater effect in ChemFET response for I- than Br- and Br- than Cl-, etc.): [30, 33]

$$ClO_4^- > SCN^- > I^- > NO_3^- > Br^- > Cl^- > HCO_3^- > CH_3CO_2^- > SO_4^{2-} > F^- > H_2PO_4^-$$

We strive to identify an approximate place in the series for HS^- by first testing a blank membrane (i.e. without an ionophore.) As previously mentioned the Hofmeister effect mechanism in not fully understood, we expect the anions respond according to the differences in lipophilicity and Gibbs energy associated with ion transfer into the membrane phase.[30, 33] By this logic, hydrosulfide may fall between iodide and chloride in the series. Following, the addition of a bambus[6]uril ionophore to the membrane is anticipated to yield preference towards the left-hand side of the series.

Experimental

General methods

Reagents and solvents were purchased from Fisher Scientific, Tokyo Chemical Industry or Sigma Aldrich. It should be noted that sodium hydrosulfide (NaSH) and ammonium sulfide evolve hydrogen sulfide gas in aqueous environments. This is toxic, and the handling of these chemicals should be done in a glove box or fume hood. Additionally, a zinc acetate quench solution and a personal H_2S monitor are encouraged when there is potential for exposure outside a glove box.

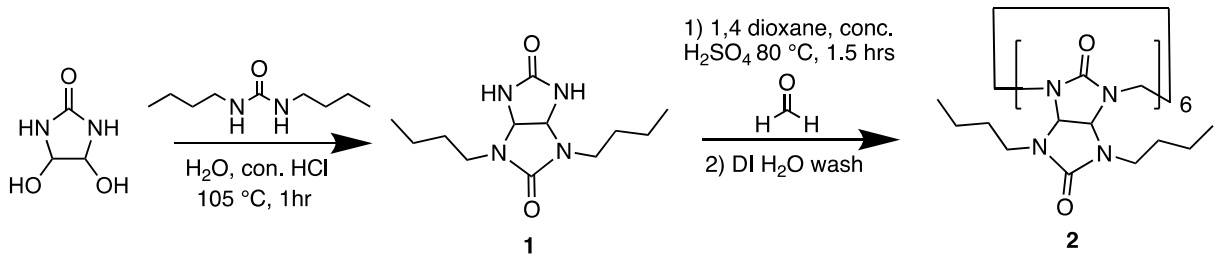

Scheme 4.1. Synthesis of the novel anion-free dodeca-n-butyl bambus[6]uril.

Receptor synthesis

N,N-dibutyl glycoluril **(n-butyl GLY)**. N,N-dibutyl urea (2.387 mg, 13.9 mmol) was added to a 35 mL solution of 4,5-dihydroxyimidozoline[27, 34] (1.631 g, 13.8 mmol) in water. To the reaction mixture, concentrated hydrochloric acid (12.1 M, 1.1 mL) was added dropwise and allowed to stir at reflux for 2 hours. The reaction mixture begins as a clear solution with insoluble chunks, and progressively yellows to a cloudy straw color. Following the allotted time, the reaction mixture was cooled to room temperature and a light-yellow solid forms. The precipitate was collected via vacuum filtration and dried under vacuum. The crude product was dissolved in acetone and purified by column chromatography (SiO_2, 95:5 EtOAc:MeOH) to produce a fluffy white solid (1.543, 44%). Structure confirmed with ^{1}H NMR (see Appendix C).

Anion-free dodeca-n-butyl bambus[6]uril **(dodeca-^{n}Bu BU[6])**. Compound **1** (1.143 g, 4.4 mmol) was added to a 30 mL mixture of paraformaldehyde (129 mg, 4.6 mmol) in 1,4 dioxane. While stirring, concentrated sulfuric acid (1 mL) was slowly added dropwise. The reaction mixture was heated at 80 ºC for 1.5 hours. The solution was initially clear with undissolved solid reagent but turned transparent and light yellow upon heating. As the reaction proceeds, the solution changes from a light yellow to a deeper straw-orange color. Following the allotted time, the solution was cooled to room temperature and precipitation occurs. The precipitate was collected

via vacuum filtration and dissolved in chloroform. The solution was taken to dryness under reduced pressure to yield an orange powder. The crude product was recrystallized in hot EtOH and acetonitrile (95:5 v/v) to yield cololess crystals (x mg, 37% yield). Structure was confirmed through mass spectrometry, ^{13}C NMR and ^{1}H NMR (see Appendix C).

Potentiometric measurements

The ChemFETs were driven by a benchtop power source, and ISFETs obtained from Winsense are used as the device base. In operation, the drain voltage (V_{ds}) is held at 617.5 mV and the drain current (I_{ds}) at 100 uA. The external reference (Ag/AgCl or Ag/Ag_2S) is held at ground, and the voltage between ground and the source (V_{gs}) terminal changes to maintain the values of V_{ds} and I_{ds}. V_{gs} is recorded as the measurement signal. NI-DAQ 6009 at a rate of 1 kHz was used for data acquisition paired with a custom Labview program for collection. Hydrosulfide experiments employed 180 seconds measurement periods to minimize electrode fouling. The other potentiometric tests were recorded for 300 seconds.

Solutions used in these experiments were prepared and used at ambient temperature. Previously reported procedures were employed to prepare samples for hydrosulfide measurement.[14] All solutions are based on a 50 mM PIPES buffer in DI water fixed to pH 7 using 4M KOH. Potassium or sodium salts containing the target anion were used to make 0.1 M stock solutions which were further diluted in 50 mL polypropylene centrifuge tubes for sensor calibration. The hydrosulfide measurements were performed in pH 8 buffer to reduce H_2S off-gas.

Electrode and membrane preparation

Silicon nitride-gated field effect transistors (FETs) were purchased from Winsense (www.winsesne.co.th, WIPS-C) and cleaned with ethanol and soaked in H_2O_2 for 10 minutes prior to functionalization. Polyvinyl chloride (PVC) and 2-nitrophenyl octyl ether (NPOE) were obtained from Fisher Scientific. Chemically selective membranes were deposited onto the FET surface by manual drop-casting. Four aliquots of 1.5 µL were applied with 15 minute drying time in between before being placed in an oven at 60 ºC for 4 hours, yielding an approximate film thickness of xyz µm. Polymer membranes were formulated as follows: A) 64 wt% NPOE (68.6 mg), 33 wt% PVC (33.2 mg), 2 wt% tetraoctylammonium nitrate (2 mg), and 1 wt% **dodeca-^{n}Bu BU[6]** (1.02 mg) in 50:50 anisole/THF (2 mL). B) 32 wt% NPOE (mg), 66 wt% PVC (69.0 mg), and 2 wt% tetraoctylammonium nitrate (2 mg) in THF (2 mL).

Ag/Ag_2S reference electrodes are employed in measurements using NaSH salt, and Ag/AgCl REs are used in all other potentiometric experiments. All REs in this report were made in-house. Procedures can be found in the Chapter III Experimental section.

Results and Discussion

Upon incorporation of 1wt% of **dodeca-^{n}Bu BU[6]** into a PVC-based membrane, sensitivity and measurement precision increased for all anions measured (Tables 4.1 and 4.3), and detection limits for Cl^- and HS^- dropped by approximately one order of magnitude. Figure 4.3 illustrates how the addition of the macrocyclic ionophore improves both detection limit and measurement precision.

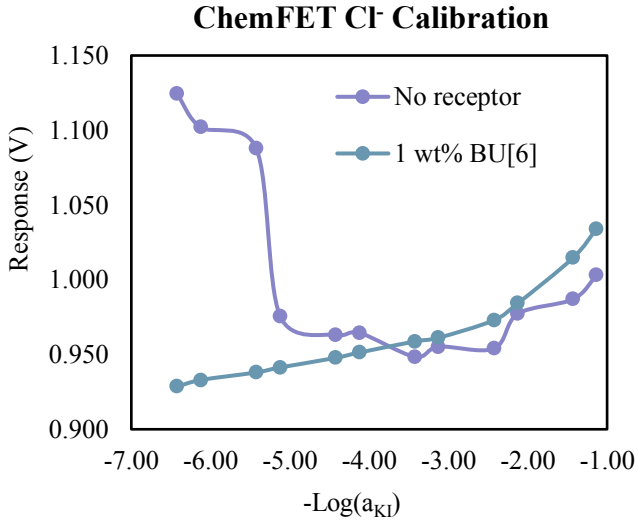

Figure 4.3 Potentiometric calibrations with and without dodeca-nBu BU[6]. Each point represents the average signal of 4 identical sensors tested in triplicate.

These results show progression towards low micromolar detection required for biomedical applications. We attribute this enhanced response to the noncovalent interactions between the membrane and the analyte. The preorganized structure of the macrocycle (Figure 4.2) yields 12 radial C-H hydrogen bond donors that stabilize the soft HS^- acceptor. It is believed that, even when membrane bound, these sites are available as described above.

During membrane optimization, it was revealed that inclusion of **dodeca-^{n}Bu BU[6]** yields a 1.0 μM detection limit for the perchlorate anion. In comparison to published work using dodecabenzyl bambus[6]uril as the ionophore, our ChemFET devices perform on par with the ~1.0 μM LoD reported.[28] This was expected due to previously reported solution-phase bambus[6]uril binding the perchlorate anion in water.[25] With a radius of approximately 240 pm, perchlorate is thought to "fit" into the binding pocket (see Figure

4.2). The impact of analyte ionic radius versus various N-substituents on bambus[6]uril functional group sensor performance will be further probed in future work.

Table 4.1. Calibration of dodeca-^{n}Bu BU[6] containing ChemFETs.

	Cl^-	HS^-
Sensitivity 1 wt% (mV/dec)	46 ± 3.3	53 ± 9.1
Detection limit (mM)	3.6 ± 3.0	0.40 ± 0.18
Sensitivity 0 wt% (mV/dec)	32 ± 6.4	30 ± 16
Detection limit (mM)	41 ± 50	3.7 ± 4.3

*Measurements are an average of 4 sensors repeated in triplicate. Standard error of the mean included.

Selectivity study

As previously mentioned, the fixed interferent method is employed to determine membrane binding preference. Using the equation below, a selectivity coefficient, $K_{A,B}^{pot}$, can be calculated:

$$K_{A,B}^{pot} = \frac{a_A}{a_B^{z_A/z_B}} \qquad 4.1$$

Where a represents the activities of the target analyte, A, and an interferent, B, at the limit of detection, and z_A and z_B are the respective charges. If $K_{A,B}^{pot} < 1$, the membrane is selective towards the target analyte, A. For example, if the selectivity coefficient is 0.10, the membrane detects 10 target anions for every 1 interferent.

Table 4.2. Results of fixed interference studies.

Interferent	Cl^-	Cys^-
Selectivity Coefficient	0.40	0.037

Notably, **dodeca-^{n}Bu BU[6]** led to selectivity towards HS^- over both chloride and thiol-containing biomolecule cysteine and (see Table 4.2). For cysteine, the high selectivity is likely due to size screening as bambus[6]uril macrocycles are geometrically suited (see figure) to bind inorganic anions. As for the preference over chloride, there could subtle C-H interactions from the n-butyl groups and quaternary ammonium cation acting favourably with the soft HS^- anion, which has been shown to be exhibit some preference for CH H-bond donors.[35] Future work could entail expanding the selectivity profile with other monovalent anions. To further define the ChemFET response, we can investigate the Hofmeister series.

Hofmeister series study

As previously stated, we are interested in observing ChemFET performance through the Hofmeister series to further characterize the behaviour of membrane-bound bambus[6]uril on potentiometric measurements. To begin, we screened the halides and perchlorate for sensitivity and determined detection limit (Table 4.3). These anions were selected due to documented bambus[6]uril halide sensitivity[36] and a recently published perchlorate ISE.[28]

Table 4.3. Detection limits for ChemFET device.

	Ionic radius (pm)	0 wt% BU (mM)	1 wt% BU (mM)
Cl^-	181	41	3.6
Br^-	196	0.36	0.22
HS^-	207	3.7	0.40
I^-	220	1.0	0.0078
ClO_4^-	240	6.1	0.0010

*BU= **dodeca-^{n}Bu BU[6]** **Ionic radii selected from Shannon, R.D. Revised Effective Ionic Radii and Systematic Studies of Interatomic Distances in Halides and Chalcogenides. *Acta Crystallographica Section A* **1976**, *32,* 751.

The detection limits given in Table 4.3 offer some insight into potential Hofmeister effects. For the membrane without ionophore, there is a deviation from the expected series as bromide displays a lower detection limit than anions may be due to cation effects in solution. When **dodeca-^{n}Bu BU[6]** is incorporated, all detection limits drop at least one order of magnitude, with the exception of bromide, indicating improved stabilization at the membrane interface. There is also a size trend with the largest anion, perchlorate, displaying the lowest detection limit. This was somewhat expected as the ~4.5Å binding pocket of bambus[6]uril hosts large anions, like perchlorate, consistently in organic and aqueous media.[28, 37] We plan to complete this study by screening additional anions, such as carbonate and fluoride, to gain a better understanding of the effect of a bambus[6]uril ionophore on both ends of the Hofmeister series. No major disruptions to the series are expected due to the size preference established through in-solution binding studies. Diminished responses are predicted for anions, such as HCO_3^- and F^- due to size and hydration energy, whereas thiocyanate should perform equal to or better than perchlorate due to similar positioning on the series.

Conclusions

In summary, we synthesized a novel bambus[6]uril receptor and investigated its anion affinity for hydrosulfide by incorporating it into a polymer membrane and performing potentiometric calibrations. This yielded a sub-millimolar detection limit and a sensor selective for hydrosulfide over chloride, cysteine, and glutathione. Additionally, we began a potentiometric Hofmeister series study with the bambus[6]uril ionophore. The bambus[6]uril-containing ChemFETs display strong sensitivity for perchlorate and iodide and have thus far shown a size trend and will be elaborated on in future work. Moving forward, bambus[6]urils should continue to be probed as components for electrochemical sensors due to their rigid structure, attractive properties in sensor membranes and potential tunability of the scaffold.

Bridge to Chapter V

The chapter above introduces bambus[6]urils as a viable ionophore for the hydrosulfide anion. This, in addition to the results of a recent Sindelar publication using this type of receptor in an ion selective electrode, illustrates the potential for the use of bambus[6]urils to as an ionophore. Chapter V reviews the work discussed in this dissertation and offers suggestions for future research directions.

CHAPTER V

CONCLUSION

Concluding Remarks

Water analysis is a crucial process for a panoply of applications, including healthcare, environmental remediation, and agriculture; therefore, the identity and concentration of aqueous anions is paramount in monitoring human and ecological well-being. While analytical approaches to sub-nanomolar anion detection exist, they require added chemicals, expertise, or complex analysis. Electrochemical sensors offer a quick, portable option for *in situ* anion monitoring; specifically, potentiometric devices have low power consumption, inexpensive production, and simple instrumentation that can be integrated into existing electronics. A robust alternative to traditional potentiometric architecture (ion-selective electrodes) is the field effect transistors (FET). FETs are a simple circuit component that, when modified with a sensing material at the gate terminal, can be used as a potentiometric platform. An effective route for functionalizing chemically selective FETs (ChemFETs) is by using a polymer membrane as the sensing material. To impart selectivity, host-guest chemistry can be used to design ionophores by employing noncovalent interactions in a similar manner to solution-state binding receptors. There has been extensive research on the construction of such receptors, and we strive to improve ionophore design inspired by receptor design principles.

This dissertation illustrates the utility of host-guest receptor design in ionophore-based potentiometric ion-selective membranes. In Chapter II, Hamilton-type receptors are employed into a ChemFET device for barbituric acid quantification. This work highlights the potential for

existing receptor molecules to be incorporated as an ionophore, and the ChemFET device performs well in media such as river water and synthetic urine. In Chapters III and IV, the hydrosulfide anion is targeted first with a simple ion exchange membrane in Ch. III. Following, a bambus[6]uril macrocycle is synthesized and implemented as a ChemFET ionophore in Ch. IV. These chapters provide insight into the crossover between electrochemical sensing and host-guest chemistry.

APPENDIX A

SUPPORTING INFORMATION FOR CHAPTER II: POTENTIOMETRIC MEASUREMENT OF BARBITURIC ACID BY INTEGRATION OF HAMILTON-TYPE RECEPTORS INTO CHEMFETS

General Procedures

^{1}H and ^{13}C NMR spectra were obtained on a Varian 500 MHz spectrometer (^{1}H 500 MHz, ^{13}C 126 MHz). ^{1}H and ^{13}C NMR chemical shifts (δ) are reported in parts per million (ppm) and referenced to residual solvent resonances($CDCl_3$: ^{1}H 7.26 ppm, ^{13}C 77.16 ppm; $(CD_3)_2CO$: ^{1}H 2.05 ppm, ^{13}C 29.84 ppm & 206.26 ppm; DMSO-d_6: ^{1}H 2.50 ppm, ^{13}C 39.52 ppm). The following abbreviations are used in describing NMR couplings: (s) singlet, (d) doublet, (t) triplet, (m) multiplet, and (b) broad. Masses for new compounds were determined with a Waters Synpat G2Si ToF spectrometer.

Potentiometric Measurements

The ChemFET device is driven by an instrumentation amplifier obtained from Winsense™ which maintains a drain voltage (V_{DS}) at 617.5 mV and the drain current (I_D) at 99.6 μA. The circuit holds an external reference electrode at ground while V_{GS}, the voltage between ground and source, is changed to maintain V_{DS} and I_D and is recorded as the measurement signal. An NI-DAQ 6009 data acquisition unit paired with a custom LabVIEW ™ program was used for monitoring and recording measurements. The signal was recorded at a rate of 1 kHz. Unless otherwise noted, each measurement was taken as the average of the signal over the 300th second of the measurement period and experiments were performed with four identical (replicate) sensors and in triplicate. Calibration of a single sensor is shown in Figure A1.

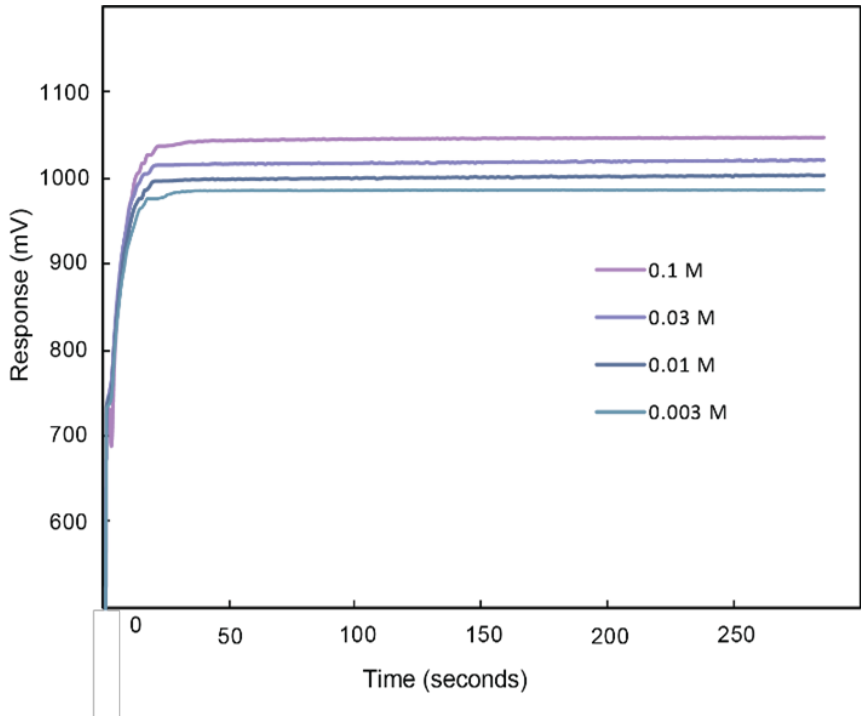

Figure A1. One ChemFETs response recorded $0.1 s^{-1}$ in solutions with varying sodium barbiturate concentrations. The sensors respond and swiftly equilibrate (approx. 90 s).

Potentiometric measurements were performed at ambient temperature in 50 mL polypropylene centrifuge tubes. The solutions were prepared fresh for each experiment by the addition of solid sodium barbiturate into 50 mM PIPES pH 7.0 buffer solution. Sodium barbiturate is insoluble at room temperature; therefore the mixture was placed on a hot plate and allowed to heat (50-70 °C) and stir until dissolved (15-30 minutes). The final stock solution has a transparent, light pink color. The neutral buffer solution was made by combining solid PIPES with deionized water. 4M KOH was added dropwise until all solid had dissolved. The pH was further adjusted using KOH until 7.0 using a pH meter. A neutral environment was used to simulate both potential biological and environmental conditions.

NMR Spectra

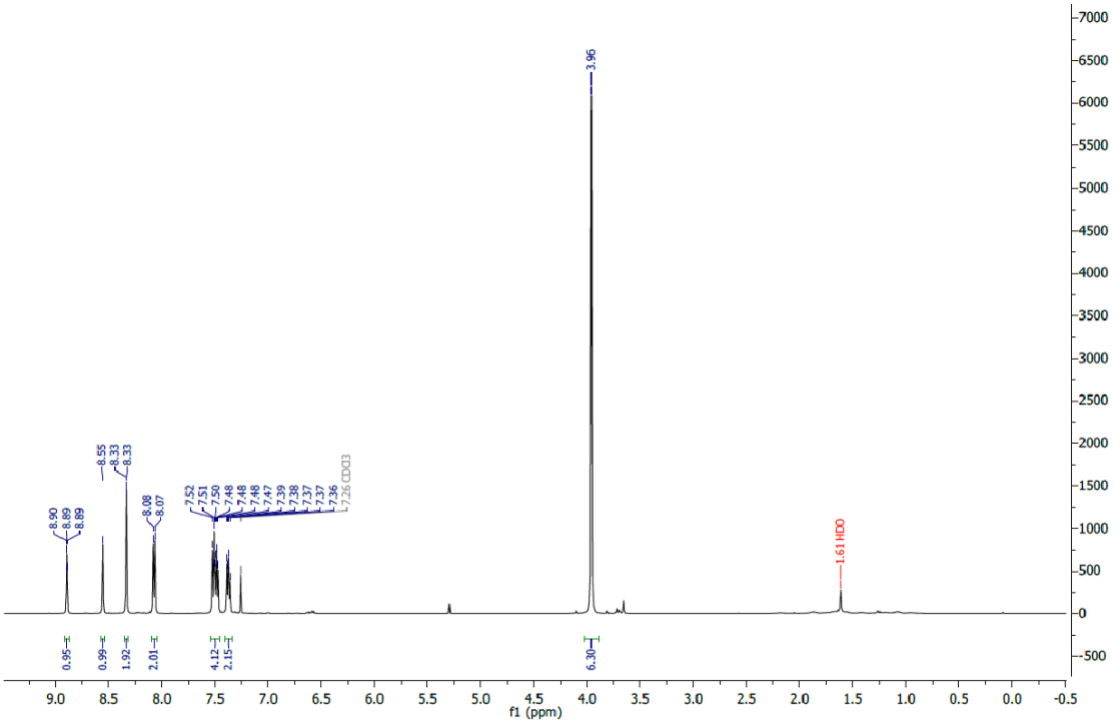

Figure A2. ^{1}H NMR spectrum of **1c**. (500 MHz, $CDCl_3$, 298 K)

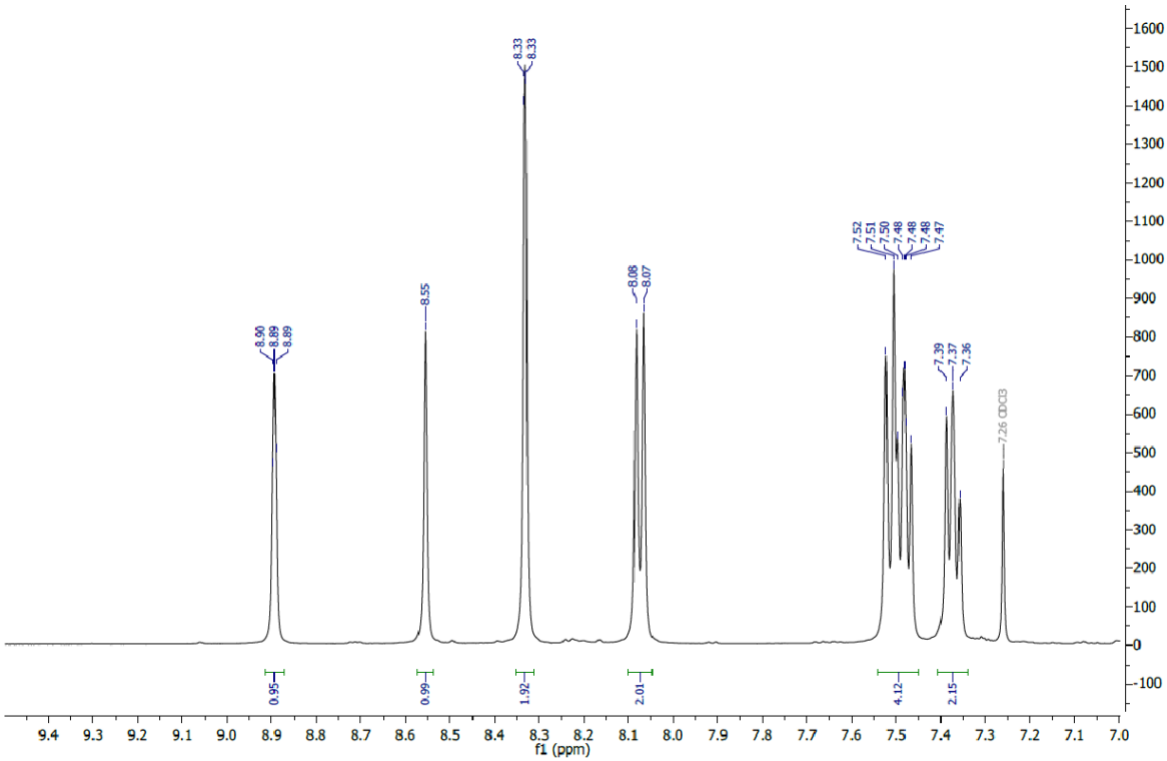

Figure A3. ^{1}H NMR spectrum of **1c**, aromatic region. (500 MHz, $CDCl_3$, 298 K)

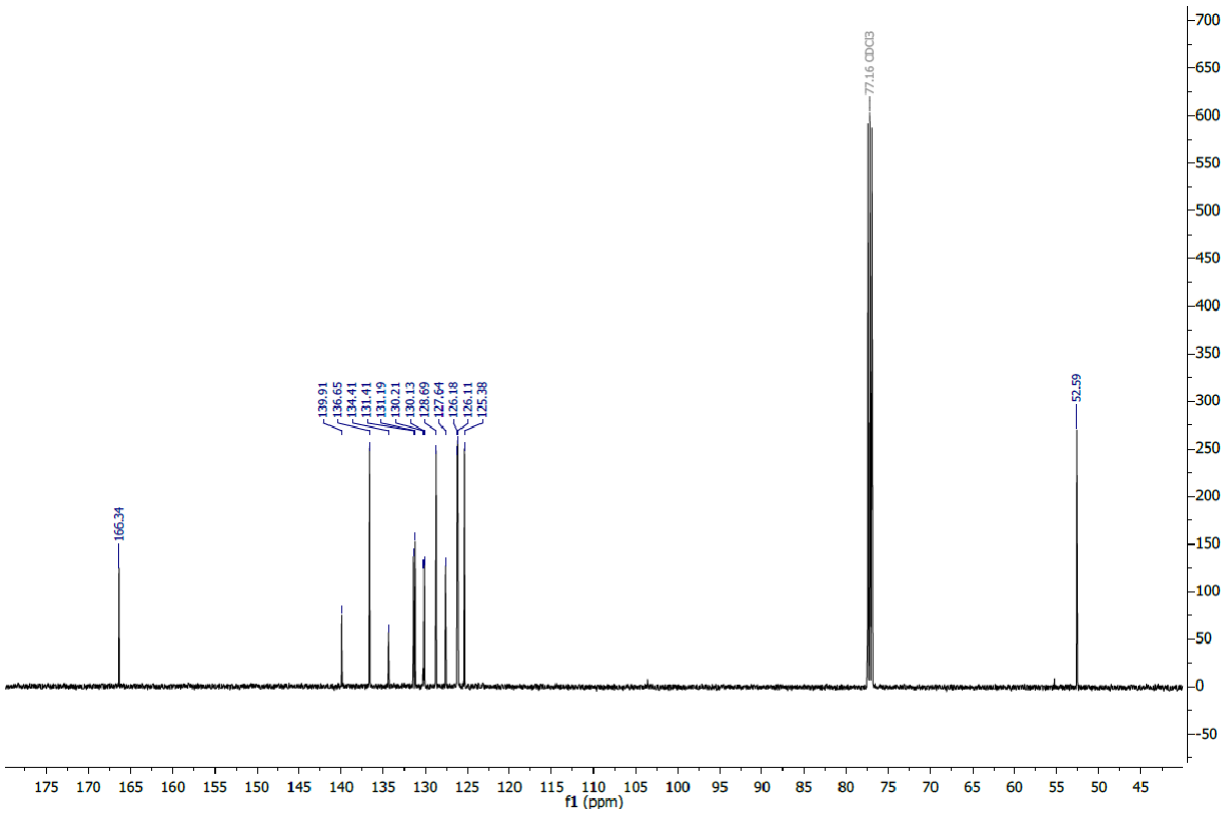

Figure A4. $^{13}C\{^{1}H\}$ NMR spectrum of **1c**. (126 MHz, $CDCl_3$, 298 K)

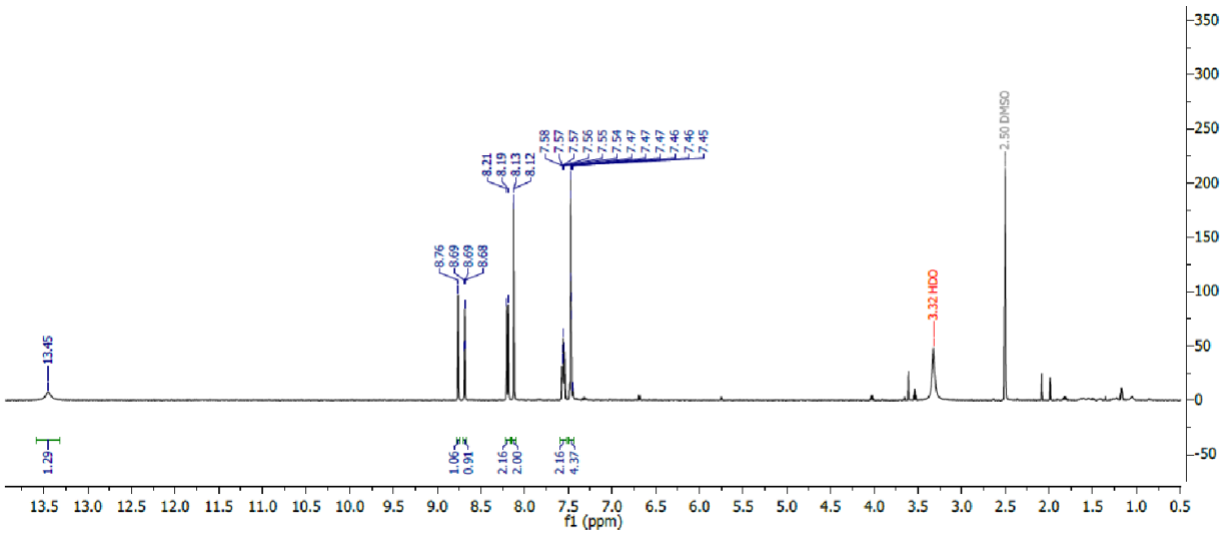

Figure A5. ^{1}H NMR spectrum of **2**. (500 MHz, *d*$_6$-DMSO, 298 K)

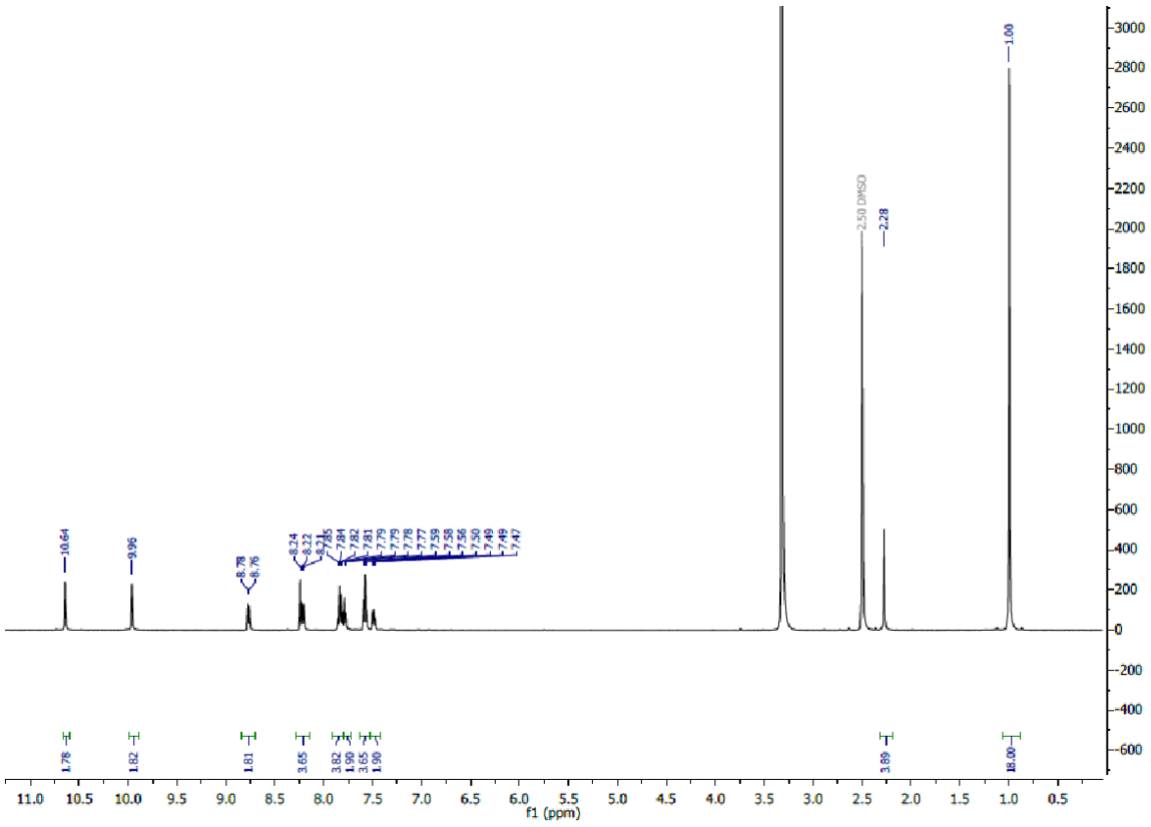

Figure A6. ^{1}H NMR spectrum of **2a**. (500 MHz, *d*$_6$-DMSOs, 298 K)

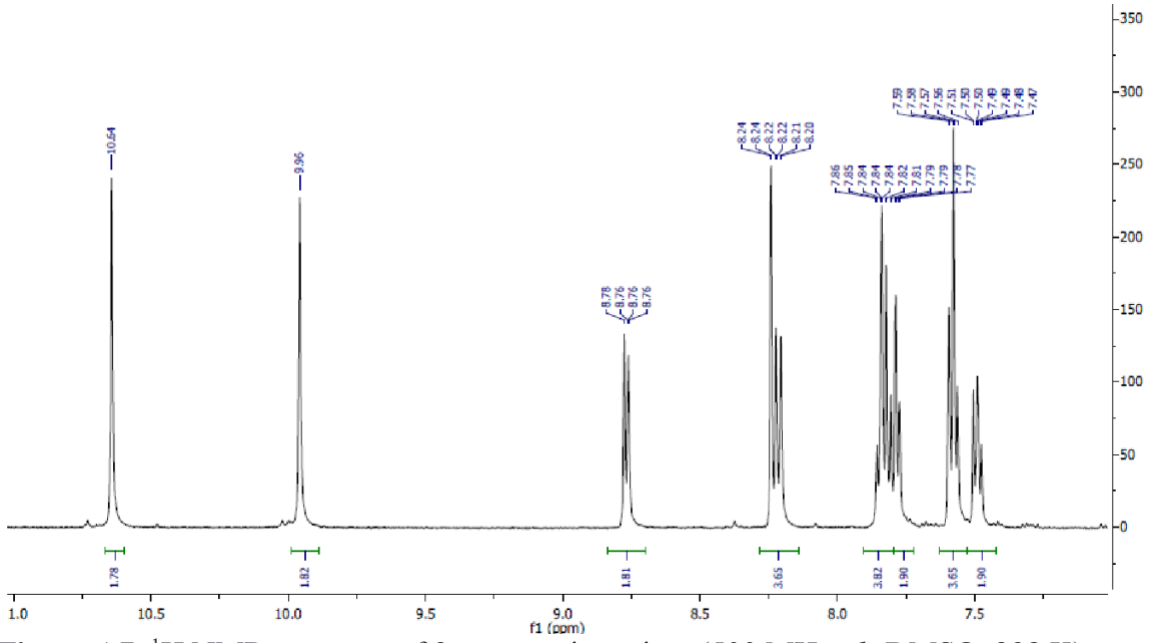

Figure A7. ^{1}H NMR spectrum of **2a**, aromatic region. (500 MHz, *d*$_6$-DMSO, 298 K)

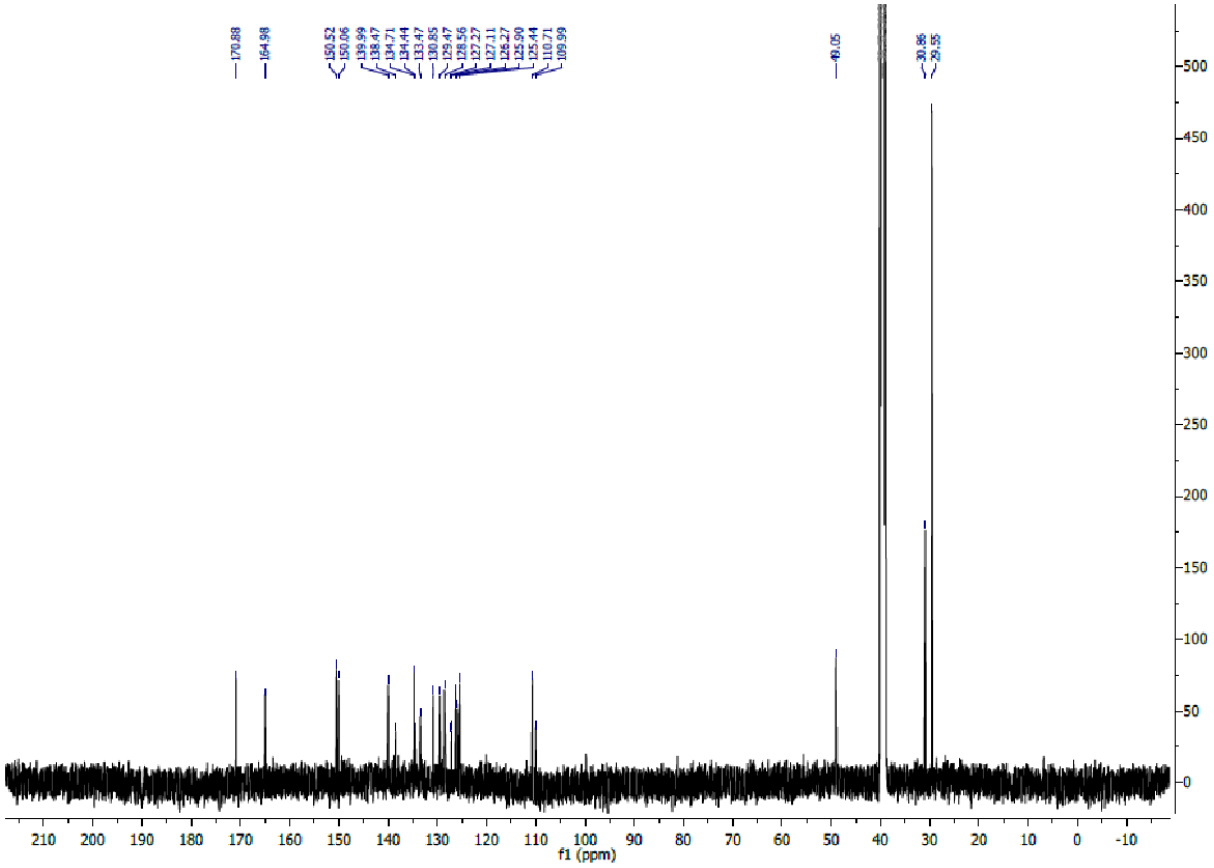

Figure A8. ^{13}C{^{1}H} NMR spectrum of **2a**. (126 MHz, *d*$_6$-DMSO, 298 K)

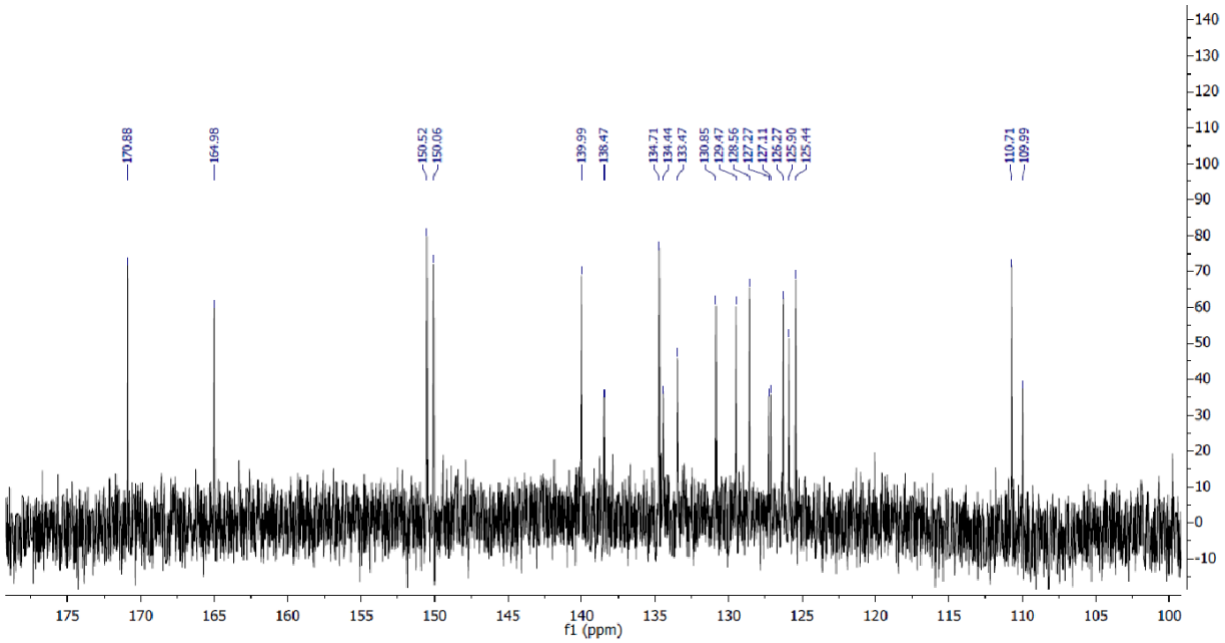

Figure A9. $^{13}C\{^{1}H\}$ NMR spectrum of **2a**, aromatic region. (126 MHz, *d*$_6$-DMSO, 298 K)

APPENDIX B

SUPPORTING INFORMATION FOR CHAPTER II: HYDROSULFIDE-SELECTIVE CHEMFETS FOR AQUEOUS H_2S/HS^- MEASUREMENT

Reference Electrode Fabrication and Characterization

Fabrication. Ag/Ag_2S reference electrodes were made as follows: Ag/Ag_2S wires were prepared by soaking silver wire (99.9%, 0.5 mm dia) in 5% ammonium sulfide solution overnight. One end of each wire was then soldered to a 20 AWG tinned copper wire and the solder joint completely encased in Loctite Marine Epoxy (1919324). To form each electrode body, a 4Å molecular sieve was pressed into the tapered end of a 1 mL polypropylene syringe body (Norm-Ject 4010.200v0). Agarose at 2 wt% was dissolved in warm 3 M KCl. 0.8 mL of this solution was poured into the syringe bodies and allowed to cool. Then the Ag/Ag_2S wire was inserted into the electrode body and the wire secured to the housing. Reference electrodes were stored in 3 M KCl overnight before their first use. Reference potentials were found to be 129-146 mV vs SCE.

Characterization. Elemental composition and surface morphology were determined by scanning electron microscopy energy dispersive X-ray spectroscopy (SEM-EDS) using a ThermoFisher Helios Hydra Plasma FIB. Images were collected with an accelerating voltage of 10 kV. Additional elemental analysis was performed using Thermo Scientific ESCALAB 250 X-ray photoelectron spectrometry (XPS) system with an Al Kα monochromated source at 20 kV. Survey spectra were taken along with high-resolution scans of Ag 3d, S 2p, and Cl 2p. Spectra were peak fit using the Thermo Scientific Avantage 4.88 software to determine surface composition.

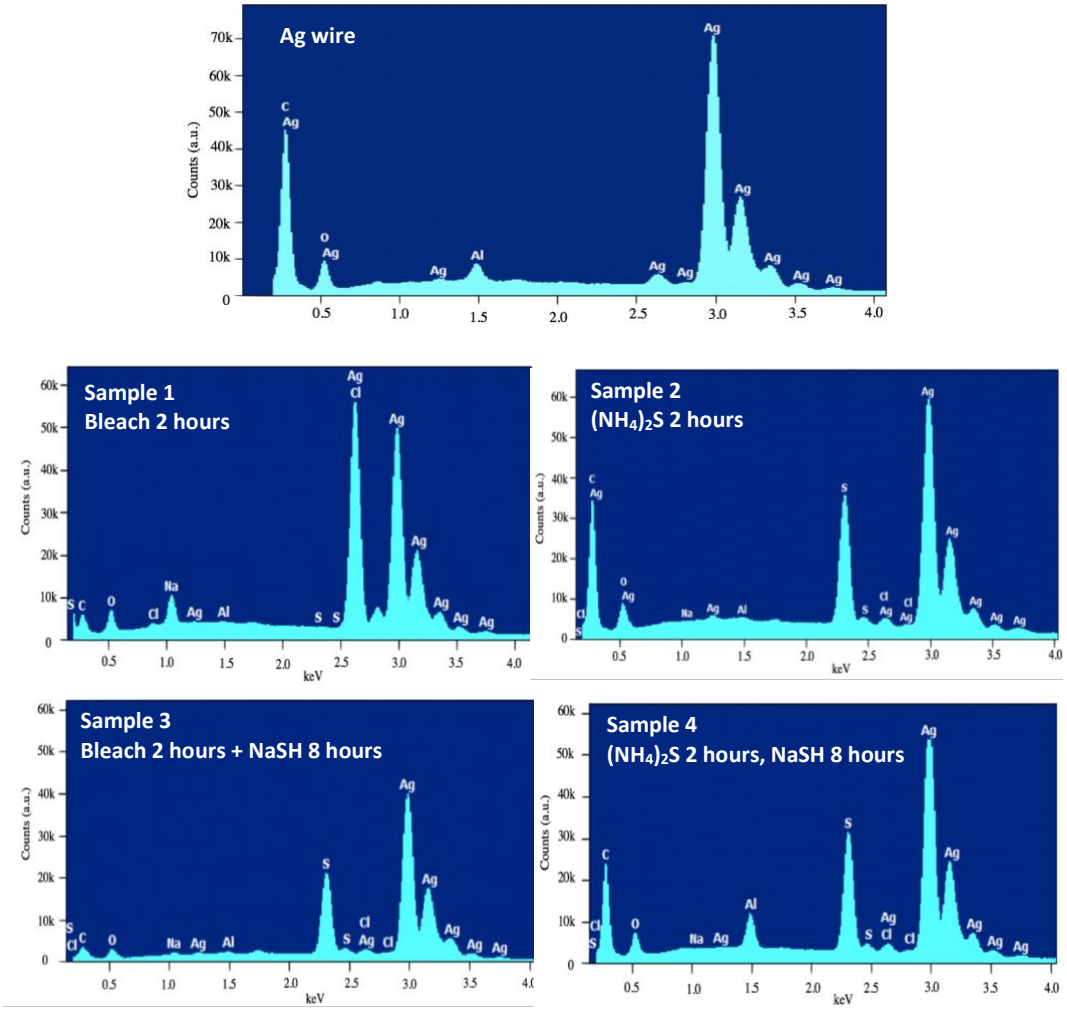

Figure B1. (top) SEM-EDS analysis of a bare 0.5 mm Ag wire. (bottom) Elemental analysis of samples 1-4.

Elemental composition	Sample 1	Sample 2	Sample 3	Sample 4
Silver	39.4	41.9	59.7	45.5
Chloride	35.8	-	-	-
Sulfur	0.25	19.1	23.8	17.8
Sodium	4.18	-	0.41	-
Oxygen*	12.8	14.7	9.97	13.4
Carbon*	7.2	19.9	5.85	19.3
Aluminum**	0.25	4.33	0.31	4.1

Table B1. Composition percentages for Ag wire samples from SEM-EDS analysis. *sample adhesive **sample mount

2. ChemFET Construction

FETs with unmodified gate oxides were purchased from WinsenseTM (www.winsense.co.th, WIPS-C). These arrive pre-bonded to small printed circuit boards on which the source and drain can be accessed via small contact pads. These pads were soldered to 20 AWG tinned copper wire and the solder joints were completely encased in Loctite Marine Epoxy (1919324) leaving only the FET surface exposed. NBR membranes were applied by drop casting using a 1-5 µL adjustable volume pipette. In general, 12 drops of approximately 1.6 µL were required to achieve the desired thickness of 100-150 µm. Drops were applied approximately 15 minutes. After drop casting, sensors were conditioned in an oven at 80 °C for at least 12 h.

Figure B2. Reference electrode (left). Red and green colored wires connected to the functionalized ChemFET (right) indicate the source and drain connections, respectively.

3. Measurement Setup.

All measurement solutions were kept sealed in 50 mL centrifuge tubes which were only opened briefly in order to insert the sensors. Special threaded caps were made which sealed the centrifuge tubes while allowing the sensors contact with the solution and while keeping sensor connections accessible (See Figure S2). Sensors were operated by analog circuits which were constructed based on the circuit diagram shown in Figure S3. The analog output (V_{GS}) was read by a data acquisition device (National Instruments DAQ 6009) which was operated by a laptop PC.

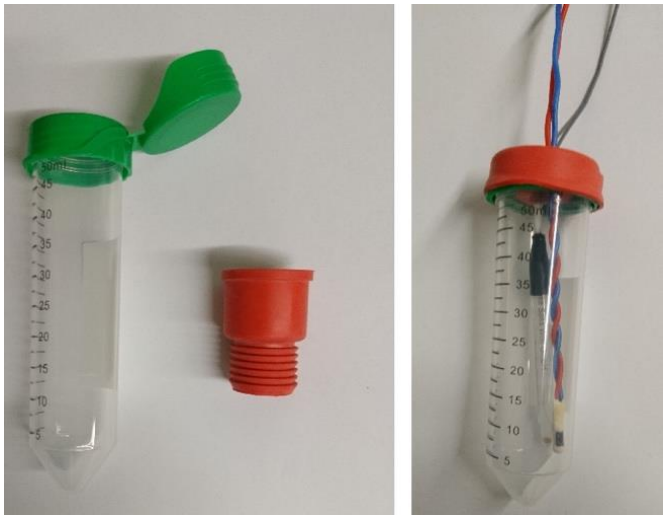

Figure B3. Centrifuge tubes used for measuring hydrosulfide-containing samples and specially modified threaded caps which enable ChemFETs and reference electrodes to pass through.

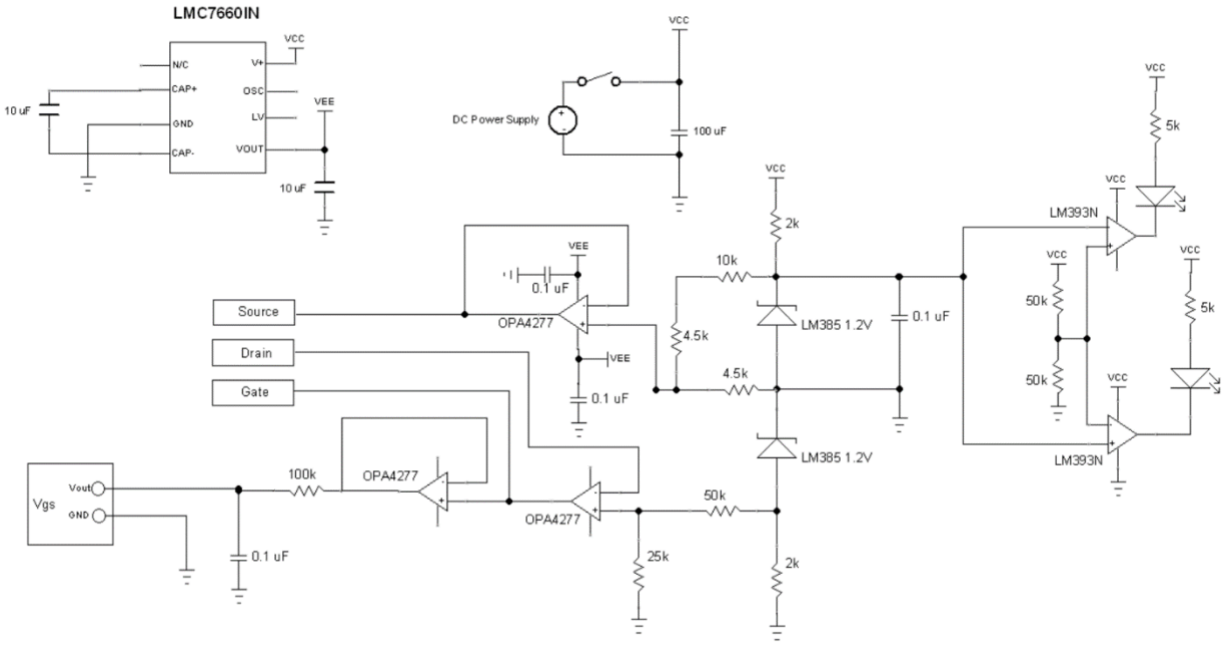

Figure B4. Circuit diagram. This circuit configuration maintains a constant drain current (I_D) of 99.6 µA and drain voltage (V_{DS}) of 617 mV in a feedback mode in which that the gate voltage (V_{GS}) necessary to maintain the constant drain current and voltage. V_{GS} is taken as the measurement signal. This circuit is based on an ISFET analog driver circuit available from Winsense (Winsense.co.th, WIPSK-CB1).

APPENDIX C

SUPPORTING INFORMATION FOR CHAPTER IV: INTEGRATION OF DODECABUTYL BAMBUS[6]URIL INTO CHEMFET FOR AQUEOUS ION DETECTION

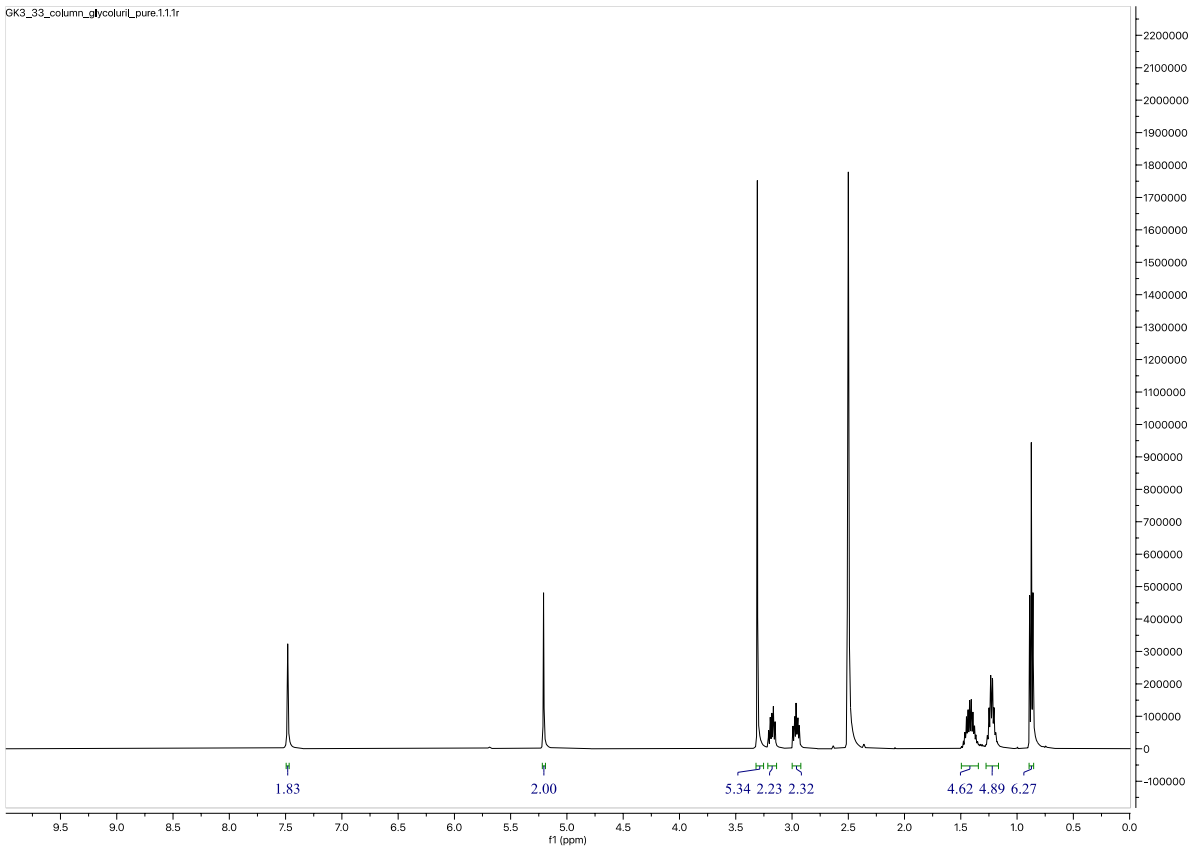

Figure C1. ^{1}H NMR spectrum of **n,n dibutyl glycoluril**. ^{1}H NMR (500 MHz, DMSO-*d*6) δ 7.48 (s, 6H), 5.21 (s, 7H), 3.18 (dt, *J* = 14.7, 7.6 Hz, 7H), 2.96 (ddd, *J* = 13.9, 8.2, 5.7 Hz, 8H), 2.45 (s, 3H), 1.42 (ddq, *J* = 20.6, 13.4, 7.0, 6.5 Hz, 15H), 1.22 (dtt, *J* = 9.6, 7.3, 3.9 Hz, 16H), 0.87 (t, *J* = 7.3 Hz, 21H).

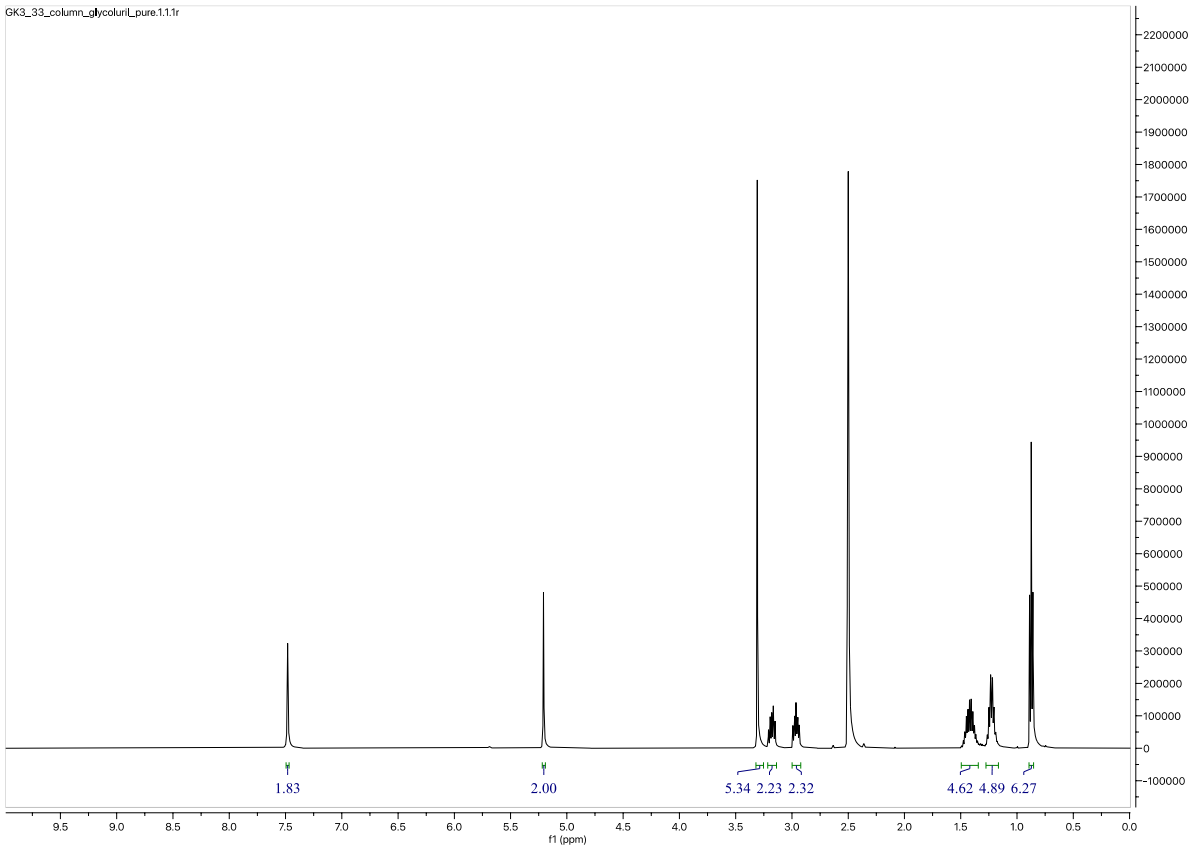

Figure C2. ^{1}H NMR (500 MHz, Chloroform-*d*) δ 5.49 (s, 4H), 4.77 (s, 4H), 3.67 (ddd, *J* = 15.3, 9.6, 6.3 Hz, 4H), 3.37 (ddd, *J* = 14.6, 9.4, 5.1 Hz, 4H), 1.76 (ddd, *J* = 14.4, 9.7, 5.7 Hz, 5H), 1.60 – 1.45 (m, 6H), 1.31 (p, *J* = 7.4 Hz, 9H), 1.25 (s, 2H), 1.22 (s, 1H), 0.93 (t, *J* = 7.3 Hz, 13H).

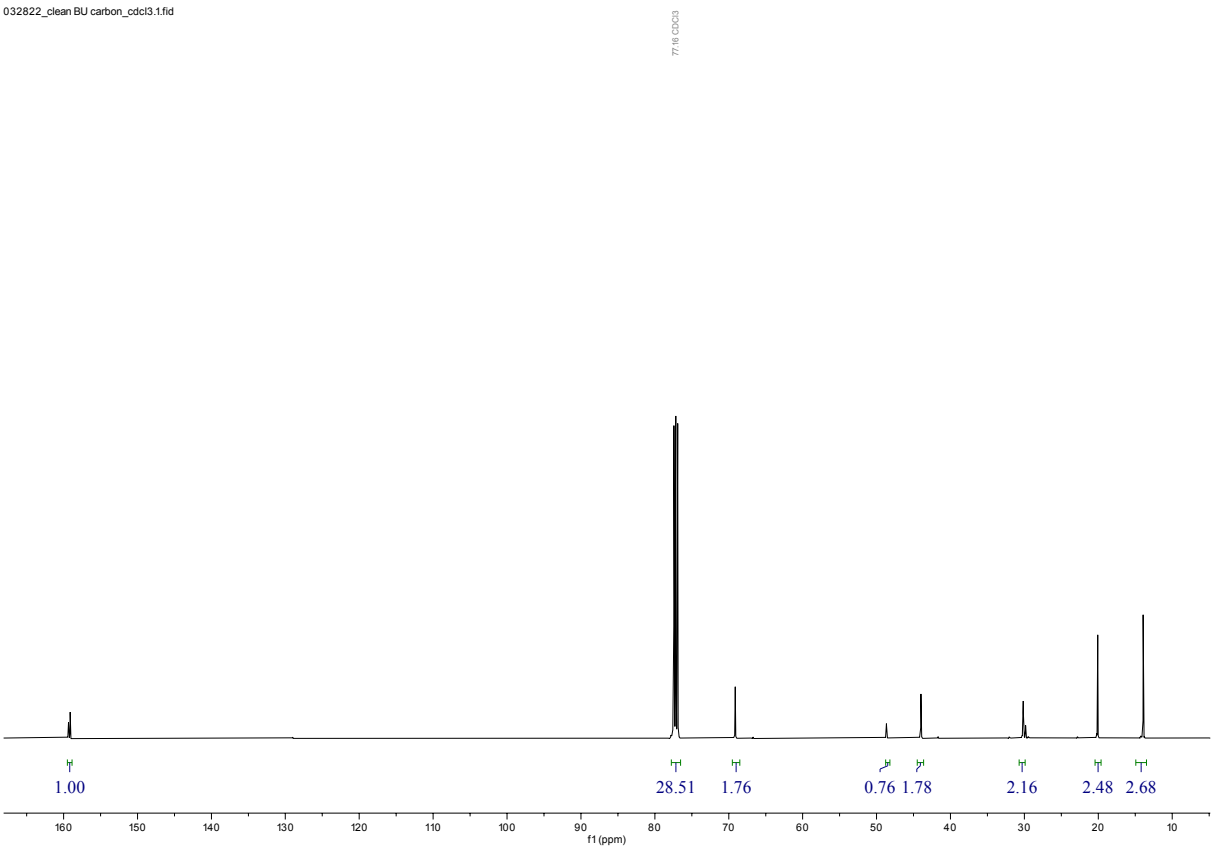

Figure C3. ^{13}C NMR spectrum of **dodecabutyl bambus[6]uril** ^{13}C NMR (126 MHz, Chloroform-*d*) δ 159.23 (d, *J* = 27.5 Hz), 69.12, 48.66, 43.99, 30.16, 20.08, 13.92.

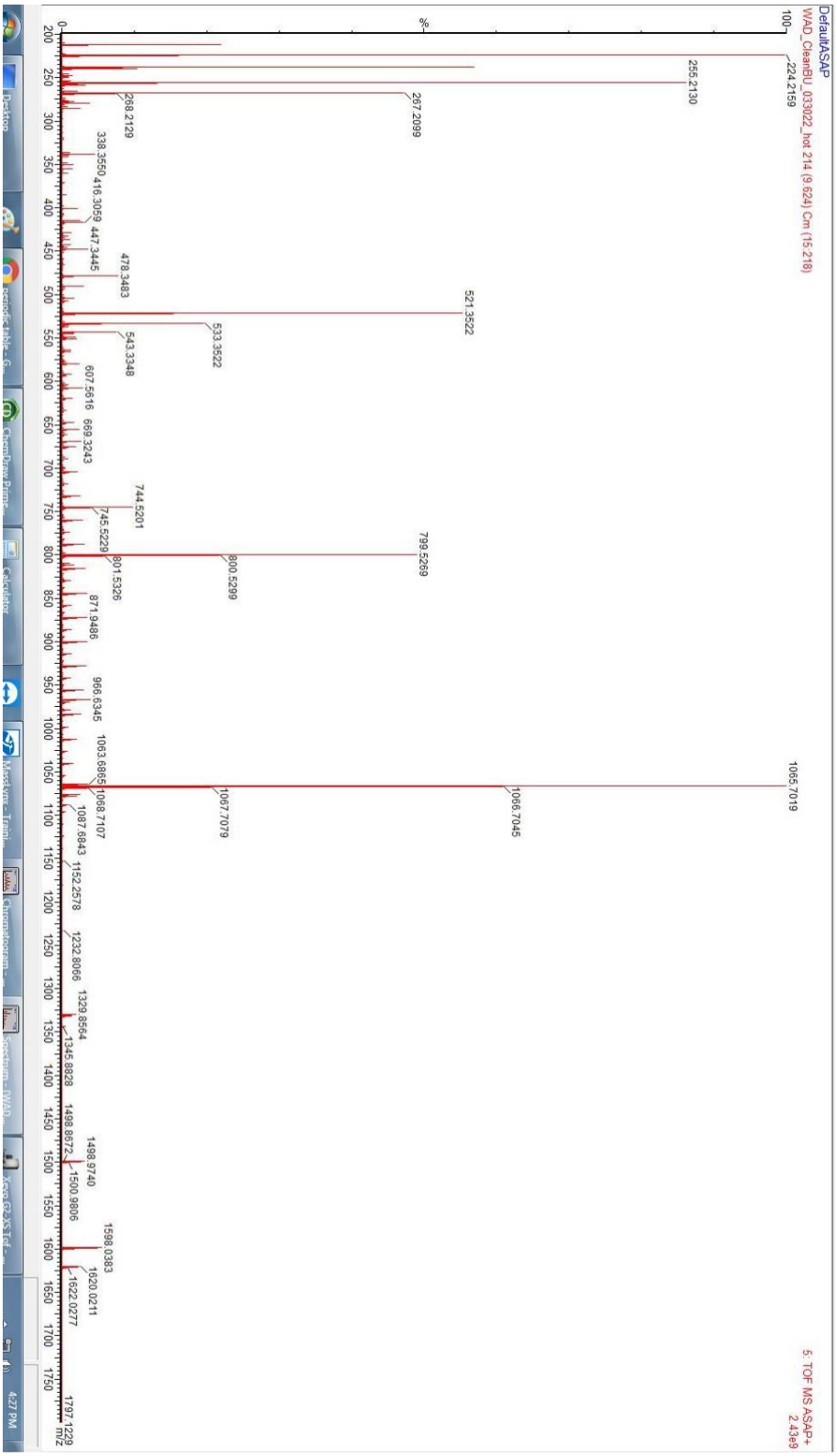

Figure C4. Mass spectrometry spectrum of **dodecabutyl bambus[6]uril**

REFERENCES CITED

Chapter I

(1) Alam, A. U.; Qin, Y.; Nambiar, S.; Yeow, J. T. W.; Howlader, M. M. R.; Hu, N. X.; Deen, M. J. Polymers and organic materials-based pH sensors for healthcare applications. *Progress in Materials Science* **2018**, *96* (April), 174-216.

(2) Stetter, J. R.; Penrose, W. R.; Yao, S. Sensors, Chemical Sensors, Electrochemical Sensors, and ECS. *Journal of The Electrochemical Society* **2003**, *150* (2), S11-S11.

(3) Chaisrirattanakua, W.; Bunjongpru, W.; Pankiew, A.; Srisuwan, A.; Jeamsaksiri, W.; Chaowicharat, E.; Thornyanadacha, N.; Pengpad, P.; Horprathum, M.; Phromyothin, D. Modification of polyvinyl chloride ion-selective membrane for nitrate ISFET sensors. *Applied Surface Science* **2020**, *512* (February), 145664-145664.

(4) Cuartero, M.; Crespo, G. A. All-solid-state potentiometric sensors: A new wave for in situ aquatic research. *Current Opinion in Electrochemistry* **2018**, *10* (April), 98-106.

(5) Kaur, B.; Erdmann, C. A.; Daniëls, M.; Dehaen, W.; Rafiński, Z.; Radecka, H.; Radecki, J. Highly Sensitive Electrochemical Sensor for the Detection of Anions in Water Based on a Redox-Active Monolayer Incorporating an Anion Receptor. *Analytical Chemistry* **2017**, *89* (23), 12756-12763.

(6) Hein, R.; Beer, P. D.; Davis, J. J. Electrochemical Anion Sensing: Supramolecular Approaches. *Chemical Reviews* **2020**, *120* (3), 1888-1935.

(7) Langton, M. J.; Serpell, C. J.; Beer, P. D. Anion recognition in water: Recent advances from a supramolecular and macromolecular perspective. *Angewandte Chemie - International Edition* **2016**, *55* (6), 1974-1987.

(8) Naskar, H.; Biswas, S.; Tudu, B.; Bandyopadhyay, R.; Pramanik, P. Voltammetric Detection of Thymol (THY) Using Polyacrylamide Embedded Graphite Molecular Imprinted Polymer (PAM@G-MIP) Electrode. *IEEE Sensors Journal* **2019**, *19* (19), 8583-8589.

(9) Karuk Elmas, Ş. N.; Ozen, F.; Koran, K.; Gorgulu, A. O.; Sadi, G.; Yilmaz, I.; Erdemir, S. Selective and sensitive fluorescent and colorimetric chemosensor for detection of CO32- anions in aqueous solution and living cells. *Talanta* **2018**, *188* (March), 614-622.; Lakshmi, P. R.; Kumar, P. S.; Elango, K. P. A simple fluorophore-imine ensemble for colorimetric and fluorescent detection of CN− and HS− in aqueous solution. *Spectrochimica Acta - Part A: Molecular and Biomolecular Spectroscopy* **2020**, *229*, 117974-117974.

(10) Habila, M. M.; Festus, E. A.; Morumda, D.; Joseph, I. FTIR and GC-MS Analysis of the Aqueous and Ethanolic Extracts of Jatropha tanjorensis Leaves. **2021**, *8* (January), 1-11.

(11) Hulanicki, A.; Glab, S.; Ingman, F. Chemical sensors definitions and classification. *Pure and Applied Chemistry* **1991**, *63* (9), 1247-1250.

(12) Murray, R. W.; Dessy, R. E.; Heineman, W. R.; Janata, J.; Seitz, R.; Ghowsi, K.; Gale, R. J. Chemical Sensors and Microinstrumentation. *Spectroscopy Letters* **1990**, *23* (4), 533-534.

(13) Janata, J. Introduction: Modern Topics in Chemical Sensing. *Chemical Reviews* **2008**, *108* (2), 327-328.

(14) Gründler, P. Chemical sensors. *ChemTexts* **2017**, *3* (4).

(15) Kassal, P.; Steinberg, M. D.; Steinberg, I. M. Wireless chemical sensors and biosensors: A review. *Sensors and Actuators, B: Chemical* **2018**, *266*, 228-245.

(16) Wang, H. Supporting Information. *Aldenderfer, Mark S., Craig, Nathan M., Speakman, Robert Jeff, and Popelka-Filcoff, Rachel S.* **1997**, *2* (1), 1-5.

(17) Hein, R.; Li, X.; Beer, P. D.; Davis, J. J. Enhanced voltammetric anion sensing at halogen and hydrogen bonding ferrocenyl SAMs. *Chemical Science* **2021**, *12* (7), 2433-2440.

(18) Karimi-Maleh, H.; Karimi, F.; Alizadeh, M.; Sanati, A. L. Electrochemical Sensors, a Bright Future in the Fabrication of Portable Kits in Analytical Systems. *Chemical Record* **2020**, *20* (7), 682-692.

(19) Berchmans, S.; Issa, T. B.; Singh, P. Determination of inorganic phosphate by electroanalytical methods: A review. *Analytica Chimica Acta* **2012**, *729*, 7-20.

(20) Bangaleh, Z.; Bagheri, H.; Ahmad, S.; Najafizadeh, P. A New Potentiometric Sensor for Determination and Screening Phenylalanine in Blood Serum Based on Molecularly Imprinted Polymer. **2019**, *18* (June 2016), 61-71. Napoli, C.; Lai, S.; Giannetti, A.; Tombelli, S.; Baldini, F.; Barbaro, M.; Bonfiglio, A. Electronic detection of DNA hybridization by coupling organic field-effect transistor-based sensors and hairpin-shaped probes. *Sensors (Switzerland)* **2018**, *18* (4).

(21) Hamed, S.; Ibba, P.; Petrelli, M.; Ciocca, M.; Lugli, P.; Petti, L. Transistor-based plant sensors for agriculture 4.0 measurements. *2021 IEEE International Workshop on Metrology for Agriculture and Forestry, MetroAgriFor 2021 - Proceedings* **2021**, 69-74.

(22) Itterheimová, P.; Bobacka, J.; Šindelář, V.; Lubal, P. Perchlorate Solid-Contact Ion-Selective Electrode Based on Dodecabenzylbambus[6]uril. *Chemosensors* **2022**, *10* (3), 1-16.

(23) Lee, C. S.; Kyu Kim, S.; Kim, M. Ion-sensitive field-effect transistor for biological sensing. *Sensors* **2009**, *9* (9), 7111-7131.

(24) Iupac. 8.3.2.4 Ion-selective field effect transistor (ISFET) devices The output signal of the. (1), 6-9.

(25) Ir, P.; Em, P. B.; Ee, F. ISFET , Theory and Practice. **2003**, (October), 1-26.

(26) Parizi, K. B.; Xu, X.; Pal, A.; Hu, X.; Philip Wong, H. S. ISFET pH Sensitivity: Counter-Ions Play a Key Role. *Scientific Reports* **2017**, *7* (3), 1-10.

(27) Yew, P. L.; Syono, M. I.; Lee, Y. H. A Solid-state Potassium Ion Sensor From Acrylic Membrane Deposited on ISFET Device. *Malaysian Journal of Chemistry* **2009**, *11* (1), 64-72.

(28) Moschou, E. A.; Chaniotakis, N. A. Chemfet based microsensors covered with ion-partitioning polymeric membranes. *Mikrochimica Acta* **2001**, *136* (3-4), 205-209.

(29) Janata, J. Electrochemical Microsensors. *Proceedings of the IEEE* **2003**, *91* (6), 864-869.

(30) Moss, S. D.; Janata, J.; Johnson, C. C. Potassium Ion-Sensitive Field Effect Transistor. **1975**, *47* (13).

(31) Liu, Y.; Yuan, T.; Zhu, J.; Qin, Y.; Jiang, D. Polymer-multiwall carbon nantubes composites for durable all solid-contact H2PO4--selective electrodes. *Sensors and Actuators, B: Chemical* **2015**, *219*, 100-104.

(32) Cao, S.; Sun, P.; Xiao, G.; Tang, Q.; Sun, X.; Zhao, H.; Zhao, S.; Lu, H.; Yue, Z. ISFET-based sensors for (bio)chemical applications: A review. *Electrochemical Science Advances* **2022**, (November 2021), 1-25.

(33) Janata, J. Historical review: Twenty years of ion-selective field-effect transistors. *The Analyst* **1994**, *119* (11), 2275-2278.

(34) Bühlmann, P.; Chen, L. D. *Ion-Selective Electrodes With Ionophore-Doped Sensing Membranes*; 2012.

(35) Sherbow, T. J.; Kuhl, G. M.; Lindquist, G. A.; Levine, J. D.; Pluth, M. D.; Johnson, D. W.; Fontenot, S. A. Hydrosulfide-selective ChemFETs for aqueous H2S/HS− measurement. *Sensing and Bio-Sensing Research* **2021**, *31*, 100394-100394.

(36) Seah, G. E. K. K.; Tan, A. Y. X.; Neo, Z. H.; Lim, J. Y. C.; Goh, S. S. Halogen Bonding Ionophore for Potentiometric Iodide Sensing. *Analytical Chemistry* **2021**, *93* (46), 15543-15549.

(37) Ganjali, M. R.; Norouzi, P.; Rezapour, M.; Faridbod, F.; Pourjavid, M. R. Supramolecular based membrane sensors. *Sensors* **2006**, *6* (8), 1018-1086.

(38) Zhu, C.; Fang, L. Mingling Electronic Chemical Sensors with Supramolecular Host-Guest Chemistry. 2014; Vol. 18, pp 1957-1964.

(39) Oshovsky, G. V.; Reinhoudt, D. N.; Verboom, W. Supramolecular chemistry in water. *Angewandte Chemie - International Edition* **2007**, *46* (14), 2366-2393.

(40) Minami, T. Design of supramolecular sensors and their applications to optical chips and organic devices. *Bulletin of the Chemical Society of Japan* **2020**, *94* (1), 24-33. DOI: 10.1246/BCSJ.20200233. Sabek, J.; Adriaenssens, L.; Guinovart, T.; Parra, E. J.; Rius, F. X.; Ballester, P.; Blondeau, P. Chloride-selective electrodes based on "two-wall" aryl-extended calix[4]pyrroles: Combining hydrogen bonds and anion-φ interactions to achieve optimum performance. *Chemistry - A European Journal* **2015**, *21* (1), 448-454.

(41) Hein, R.; Borissov, A.; Smith, M. D.; Beer, P. D.; Davis, J. J. A halogen-bonding foldamer molecular film for selective reagentless anion sensing in water. *Chemical Communications* **2019**, *55* (33), 4849-4852.

(42) Lee, H. K.; Oh, H.; Nam, K. C.; Jeon, S. Urea-functionalized calix[4]arenes as carriers for carbonate-selective electrodes. *Sensors and Actuators, B: Chemical* **2005**, *106* (1 SPEC. ISS.), 207-211.

(43) Zahran, E. M.; Hua, Y.; Lee, S.; Flood, A. H.; Bachas, L. G. Ion-selective electrodes based on a pyridyl-containing triazolophane: Altering halide selectivity by combining dipole-promoted cooperativity with hydrogen bonding. *Analytical Chemistry* **2011**, *83* (9), 3455-3461.

Chapter II

(1) Hein, R.; Beer, P. D.; Davis, J. J. Electrochemical Anion Sensing: Supramolecular Approaches. *Chemical Reviews* **2020**, *120* (3), 1888-1935.

(2) Busschaert, N.; Caltagirone, C.; Van Rossom W.; Gale, W.; Applications of Supramolecular Anion Recognition. *Chemical Reviews* **2015** *155*, 8038-8155.

(3) Zahran, E. M.; Hua, Y.; Lee, S.; Flood, A. H.; Bachas, L. G. Ion-selective electrodes based on a pyridyl-containing triazolophane: Altering halide selectivity by combining dipole-promoted cooperativity with hydrogen bonding. *Analytical Chemistry* **2011**, *83* (9), 3455-3461.

(4) Kristofco, L. A.; Brooks, B. W. Global scanning of antihistamines in the environment: Analysis of occurrence and hazards in aquatic systems. *Science of the Total Environment* **2017**, *592*, 477-487.

(5) Peschka, M.; Eubeler, J. P.; Knepper, T. P. Occurrence and Fate of Barbiturates in the Aquatic Environment. *Environmental Science and Technology* **2006**, *40*, 7200-7206.

(6) Pavlidakey, P. G.; Brodell E. E.; Helms, S. E. Diphenhydramine as an alternative local anesthetic agent. *Journal of Clinical and Aesthetic Dermatology* **2009**, *10,* 37-40.

(7) Gottschall, N.; Topp, E.; Metcalfe, C.; Edwards, M.; Payne, M.; Kleywegt, S.; Russell P.; Lapen, D. R. Pharmaceutical and personal care products in groundwater, subsurface drainage, soil, and wheat grain, following a high single application of municipal biosolids to a field. *Chemosphere* **2012**, *87*,194-203.

(8) Sabourin, L.; Duenk, P.; Bonte-Gelok, S.; Payne, M.; Lapen D. R.; Topp E. Uptake of pharmaceuticals, hormones and parabens into vegetables grown in soil fertilized with municipal biosolids *Science of the Total Environment* **2012**, *431*, 233-236.

(9) Bagsby, C.; Saha, A.; Goodin, G.; Siddiqi, S.; Farone, M.; Farone, A.; Kline, P. C. Stability of pentobarbital in soil, *Journal of Environmental Science and Health Part B*. **2018**, *53*, 207-213.

(10) Zdrachek E.; Bakker E. Potentiometric Sensing. *Analytical Chemistry* **2019**, *91,* 2-26.

(11) Bobacka, J.; Ivaska, A.; Lewenstam, A. Potentiometric Ion Sensors. *Chemical Reviews* **2008**, *108*, 329-51.

(12) Langton, M. J.; Serpell, C. J.; Beer, P. D. Anion recognition in water: Recent advances from a supramolecular and macromolecular perspective. *Angewandte Chemie - International Edition* **2016**, *55* (6), 1974-1987. DOI: 10.1002/anie.201506589.

(13) Kubik, S. Anion recognition in water. *Chemical Society Reviews* **2010**, *39,* 3648-3663.

(14) a) Lehn, J. M. Supramolecular chemistry: Where from? Where to? *Chemical Society Reviews* **2017**, *46*, 2378-2379. b) Young, M. C.; Liew E.; Hooley, R. J. Colorimetric barbiturate sensing with hybrid spin crossover assemblies. *Chemical Communications* **2014**, *50*, 5043-5045.

(15) Ganjali, M.R.; Norouzi, P.; Rezapour, M.; Faridbod, F.; Pourjavid, M.R. Supramolecular Based Membrane Sensors. *Sensors (Basel)* **2006**, 6(*8*), 1018–86.

(16) Zhu C.; Fang, L. Mingling Electronic Chemical Sensors with Supramolecular Host-Guest Chemistry. *Current Organic Chemistry* **2014**, *18*, 1957-1964.

(17) Borissov, A.; Marques, I.; Lim, J. Y. C.; Félix, V.; Smith, M. D. Beer, P. D. Anion Recognition in Water by Charge-Neutral Halogen and Chalcogen Bonding Foldamer Receptors. *Journal of the American Chemical Society* **2019**, *141,* 4119-4129.

(18) Friščić, T. Supramolecular concepts and new techniques in mechanochemistry: cocrystals, cages, rotaxanes, open metal–organic frameworks. *Chemical Society Reviews* **2012**, *41*, 3493- 3510.

(19) Cornes, S. P. Sambrook, M. R.; Beer, P. D. Selective perrhenate recognition in pure water by halogen bonding and hydrogen bonding alpha-cyclodextrin based receptors. *Chemical Communications* **2017**, *53*, 3866-3869.

(20) Chang S. K.; Hamilton, A. D. Molecular Recognition of Biologically Interesting Substrates: Synthesis of an Artificial Receptor for Barbiturates Employing Six Hydrogen Bonds. *Journal of the American Chemical Society* **1988**, *110*, 1318-1319.

(21) McGrath J. M.; Pluth, M. D. Linear Free Energy Relationships Reveal Structural Changes in Hydrogen-Bonded Host−Guest Interactions. *Journal of Organic Chemistry* **2014**, *79*,11797-11801.

(22) Berl, V.; Schmutz, M.; Krische, M. J.; Khoury, R. G.; Lehn, J. M. Supramolecular Polymers Generated from Heterocomplementary Monomers Linked through Multiple Hydrogen-Bonding Arrays—Formation, Characterization, and Properties. *Chemistry: A European Journal* **2002**, *8,* 1227-1244.

(23) Ali, M.; Hasenöhrl, D. H.; Zeininger, L.; Müllner, A. R. M.; Peterlik, H.; Hirsch, A. Hamilton Receptor-Mediated Self-Assembly of Orthogonally Functionalized Au and TiO2 Nanoparticles. *Helvetica Chimica Acta* **2019**, *102,* e1900015.

(24) Prasad, B. B.; Lakshmi, D. Barbituric Acid Sensor Based on Molecularly Imprinted Polymer-Modfied Hanging Mercury Drop Electrode. *Electroanalysis* **2005**, *17*, 1260-1268.

(25) Patel, A. K.; Sharma. P. S.; Prasad, B. B. Voltammetric Sensor for Barbituric Acid Based on a Sol-Gel Derivated Molecular Imprinted Polymer Brush Grafted to Graphite Electrode. *Journal of International Pharmaceutics* **2009**, *371*, 47-55.

(26) Aman, T.; Khan, I. U.; Praveen, Z. Spectrophotometric Determination of Barbituric Acid. *Analytical Letters* **1997**, *30*, 2765-2777.

(27) Ibraheem, B. B. Spectrophotometric determination of barbituric acid by coupling with diazotized nitroanilines. *Rafidian Journal of Science* **2011**, *22*, 56-71.

(28) Zarei, A. R.; Gholamian, F. Development of a dispersive liquid–liquid microextraction method for spectrophotometric determination of barbituric acid in pharmaceutical formulation and biological samples. *Analytical Biochemistry* **2011**, *412*, 224-228.

(29) Liftshits, L. M.; Zeller, M.; Campana C. F.; Klosterman, J. K. Metal-Organic Frameworks as Molecular Templates for Directing Aromatic Motifs. *Crystal Growth and Design* **2017**, *17*, 5449.

(30) D. T. Seidenkranz, J. M. McGrath, L. N. Zakharov and M. D. Pluth. Supramolecular Bidentate Phosphine Ligand Scaffolds from Deconstructed Hamilton Receptors. *Chemical Communications* **2017**, *53*, 561-564.

(31) Chen, Y. T.; Sarangadharan, I.; Sukesan, R.; Hseih, C. Y.; Lee, G. Y.; Chyi J. I.; Wang, Y. L. High-field modulated ion-selective field-effect-transistor (FET) sensors with sensitivity higher than the ideal Nernst sensitivity. *Scientific Reports* **2018**, *8*, 1-11.

(32) Buck, R.P.; Lindner, E. Recommendations for Nomenclature of Ion-Selective Electrodes. *Pure and Applied Chemistry* **1994**, *12* (66), 2527-2536.

Chapter III

(1) Driver, L.; Freedman, E. Report to Congress on Hydrogen Sulfide Air Emissions Associated with the Extraction of Oil and Natural Gas. U.S. Environmental Protection Agency, Office of Air Quality Planning and Standards. **1993**.

(2) Dry Natural Gas Production. U.S. Department of Energy. (Accessed October 2, **2019**).

(3) Wang, R. Physiological Implications of Hydrogen Sulfide: A Whiff Exploration That Blossomed. *Physiology Reviews* **2012**, 92, 791-896.

(4) Yang, G.; Wu, L.; Jiang, B.; Yang, W.; Qi, J.; Cao, K.; Meng, Q.; Mustafa, A.; Zhang, S.; Snyder, S.; Wang, R. H_2S as a Physiologic Vasorelaxant: Hypertension in Mice with Deletion of Cystathionine γ-Lyase. *Science* **2008**, *322,* 587-90.

(5) Feng, X.; Chen, Y.; Zhao, J.; Tang, C.; Jiang, Z.; Geng, B. Hydrogen sulfide from adipose tissue is a novel insulin resistance regulator. *Biochemical and Biophysical Research Communications* **2009**, *380*, 153-9.

(6) Whiteman, M.; Cheung, N.S.; Zhu, Y.-Z.; Chu, S.H.; Siau, J.L.; Wong, B.S.; Armstrong, J.S.; Moore, P.K. Hydrogen sulphide: a novel inhibitor of hypochlorous acid-mediated oxidative damage in the brain? *Biochemical and Biophysical Research Communications* **2005**, *326*, 794-8.

(7) Wang, R. Two's company, three's a crowd: can H2S be the third endogenous gaseous transmitter? *The Federation of American Societies for Experimental Biology Journal* **2002**, *16*, 1792-8.

(8) Wang, R. The Gasotransmitter Role of Hydrogen Sulfide, *Antioxidants and Redox Signalling* **1994,** *5*, 493-501.

(9) Lin, V.S.; Chen, W.; Xian, M.; Chang, C.J. Chemical probes for molecular imaging and detection of hydrogen sulfide and reactive sulfur species in biological systems. *Chemical Society Reviews* **2015**, *44*, 4596-618.

(10) Fogo, J.K.; Popowsky, M. Spectrophotometric Determination of Hydrogen Sulfide, *Analytical Chemistry* **1949**, *21,* 732-4.

(11) Montoya, L.A.; Pearce, T.F.; Hansen, R.J.; Zakharov, L.N.; Pluth, M.D. Development of Selective Colorimetric Probes or Hydrogen Sulfide Based on Nucleophilic Aromatic Substitution. *Journal of Organic Chemistry* **2013**, *78*, 6550-7.

(12) Pandey, S.K.; Kim, K.-H.; Tang, K.-T. A review of sensor-based methods for monitoring hydrogen sulfide. *Trends in Analytical Chemistry* **2012**, *32*, 3287-99.

(13) Pandey, S.K.; Kim, K.-H. A Review of Methods for the Determination of Reduced Sulfur Compounds (RSCs) in Air. *Environmental Science and Technology* **2009**, *43,* 3020-9.

(14) Zdrachek, E.; Bakker, E. Potentiometric Sensing. *Analytical Chemistry* **2019**, *91*, 2-26.

(15) Sizov, A.S.; Trul, A.A.; Chekusova, V.; Borshchev, O.V.; Vasiliev, A.A.; Agina, E.V.; Ponomarenko, S. Highly Sensitive Air-Stable Easily Processable Gas Sensors Based on Langmuir–Schaefer Monolayer Organic Field-Effect Transistors for Multiparametric H_2S and NH_3 Real-Time Detection. *ACS Applied Materials and Interfaces* **2018**, *104*, 3831-41.

(16) Shivaraman, M.S. Detection of H_2S with Pd-gate MOS field-effect transistors, *Journal of Applied Physics Phys* **1976**, *47,* 3592-3.

(17) Lundström, I.; Armgarth, M.; Spetz, A.; Winquist, F. Gas sensors based on catalytic metal-gate field-effect devices. *Sensors and Actuators*, **1986**,10399-421.

(18) Lloyd Spetz, A.; Unéus, L.; Svenningstorp, H.; Tobias, P.; Ekedahl, L.-G.; Larsson, O. Göras, A.; Savage, S.; Harris, C.; Mårtensson, P.; Wigren, R.; Salomonsson, P.; Häggendahl, B.; Ljung, P.; Mattsson, M.; Lundström, I. SiC Based Field Effect Gas Sensors for Industrial Applications. *Physica Status Solidi (a)* **2001**, *185*, 15-25.

(19) Bergveld, P. Thirty years of ISFETOLOGY: What happened in the past 30 years and what may happen in the next 30 years. *Sensors and Actuators B-Chemical* **2003**, *88*, 1-20.

(20) Kaisti, M. Detection principles of biological and chemical FET sensors. *Biosensing and Bioelectronics* **2017**, *98*, 437-48.

(21) Janata, J. Potentiometric Sensors. *Principles of Chemical Sensors* **2009**, p. 119-99.

(22) Iskierko, Z.; Noworyta, K.; Sharma, P.S. Molecular recognition by synthetic receptors: Application in field-effect transistor based chemosensing. *Biosensing and Bioelectronics* **2018**, *109,* 50-62.

(23) Bobacka, J.; Ivaska, A.; Lewenstam, A. Potentiometric Ion Sensors. *Chemical Reviews* **2008**, *108*, 329-51.

(24) Hughes, M.N.; Centelles, M.N.; Moore, K.P. Making and working with hydrogen sulfide: The chemistry and generation of hydrogen sulfide in vitro and its measurement in vivo: A review. *Free Radical Biology and Medicine* **2009**, 47, 1346-53.

(25) Hartle, M.D.; Pluth, M.D. A practical guide to working with H2S at the interface of chemistry and biology. *Chemical Society Reviews* **2016,** *45*, 6108-17.

(26) Ebdon, L.; Braven, J.; Frampton, N.C. Nitrate-selective electrodes with polymer membranes containing immobilised sensors. *Analyst* **1990,** *115,*189-93.

(27) Antonisse, M.M.G.; Lugtenberg, R.J.W.; Egberink, R.J.M.; Engbersen, J.F.J.; Reinhoudt, D.N. Durable nitrate-selective chemically modified field effect transistors based on new polysiloxane membranes. *Analytica Chimica Acta* **1996,** *332*, 123-9.

(28) Stauthamer, W.P.R.V.; Engbersen, J.F.J.; Verboom, W.; Reinhoudt, D.N. Influence of plasticizer on the selectivity of nitrate-sensitive CHEMFETs. *Sensors and Actuators B-Chemical* **1994,** *17*, 197-201.

(29) Cao, A.; Mescher, M.; Bosma, D.; Klootwijk, J.H.; Sudhölter, E.J.R.; Smet, L.C.P.M. Ionophore-Containing Siloprene Membranes: Direct Comparison between Conventional Ion-Selective Electrodes and Silicon Nanowire-Based Field-Effect Transistors. *Analytical Chemistry* **2015,** *87*, 1173-9.

(30) Nielsen, H.J; Hansen, E.H. New nitrate ion-selective electrodes based on quaternary ammonium compounds in nonporous polymer membranes. *Analytica Chimica Acta* **1976**, *85*, 1-16.

(31) Hartle, M.D.; Meininger, D.J.; Zakharov, L.N.; Tonzetich, L.N.; Pluth, M.D. NBu_4SH provides a convenient source of HS^- soluble in organic solution for H_2S and anion-binding research. *Dalton Transactions* **2015**, *44*, 19782-5.

(32) Moser, N.; Lande, T.S.; Toumazou, C.; Georgiou, P. ISFETs in CMOS and Emergent Trends in Instrumentation: A Review. *IEEE Sensors Journal* **2016,** *166*, 496-514.

(33) Buck, R.P.; Lindner, E. Recommendations for Nomenclature of Ion-Selective Electrodes. *Pure and Applied Chemistry* **1994**, *12* (66), 2527-2536.

(34) Hartle, M.D.; Hansen, R.J.; Tresca, B.W.; Prakel, S.S.; Zakharov, L.N.; Haley, M.M.; Pluth, M.D.; Johnson, D.W. A Synthetic Supramolecular Receptor for the Hydrosulfide Anion. *Angewandte Chemie International Edition* **2016,** *55*, 11480-4.

(35) Lau, N.; Zakharov, L.N.; Pluth, M.D. Modular tripodal receptors for the hydrosulfide (HS^-) anion. *Chemical Communications* **2018,** *54*, 2337-40.

Chapter IV

(1) Hartle, M. D.; Hansen, R. J.; Tresca, B. W.; Prakel, S. S.; Zakharov, L. N.; Haley, M. M.; Pluth, M. D.; Johnson, D. W. A Synthetic Supramolecular Receptor for the Hydrosulfide Anion. *Angewandte Chemie - International Edition* **2016**, *55* (38), 11480-11484.

(2) Jiang, Y.; Jin, D.; Li, Y.; Yan, X.; Chen, L. A near-infrared fluorescent probe for rapid and selective detection of hydrosulfide and imaging in live cells. *Research on Chemical Intermediates* **2017**, *43* (5), 2945-2957.

(3) Havel, V.; Yawer, M. A.; Sindelar, V. Real-time analysis of multiple anion mixtures in aqueous media using a single receptor. *Chemical Communications* **2015**, *51* (22), 4666-4669. Langton, M. J.; Serpell, C. J.; Beer, P. D. Anion recognition in water: Recent advances from a supramolecular and macromolecular perspective. *Angewandte Chemie - International Edition* **2016**, *55* (6), 1974-1987. Zahran, E. M.; Hua, Y.; Li, Y.; Flood, A. H.; Bachas, L. G. Triazolophanes: A new class of halide-selective lonophores for potentiometrie sensors. *Analytical Chemistry* **2010**, *82* (1), 368-375.

(4) Hartle, M. D.; Pluth, M. D. A practical guide to working with H2S at the interface of chemistry and biology. *Chemical Society Reviews* **2016**, *45* (22), 6108-6117. DOI: 10.1039/c6cs00212a.

(5) Shen, X.; Peter, E. A.; Bir, S.; Wang, R.; Kevil, C. G. Analytical measurement of discrete hydrogen sulfide pools in biological specimens. *Free Radical Biology and Medicine* **2012**, *52* (11-12), 2276-2283.

(6) Mitchell, E. J.; Beecroft, A. J.; Martin, J.; Thompson, S.; Marques, I.; Félix, V.; Beer, P. D. Hydrosulfide (HS −) Recognition and Sensing in Water by Halogen Bonding Hosts. *Angewandte Chemie* **2021**, *133* (45), 24250-24255.

(7) Lau, N.; Zakharov, L. N.; Pluth, M. D. Modular tripodal receptors for the hydrosulfide. *Chemical Communications* **2018**. DOI: 10.1039/C7CC09405A.

(8) Vázquez, J.; Sindelar, V. Supramolecular binding and release of sulfide and hydrosulfide anions in water. *Chemical Communications* **2018**, *54* (46), 5859-5862. DOI: 10.1039/c8cc00470f.

(9) Bakker, E.; Telting-Diaz, M. Electrochemical sensors. *Analytical Chemistry* **2002**, *74* (12), 2781-2800.. Fakih, I.; Durnan, O.; Mahvash, F.; Napal, I.; Centeno, A.; Zurutuza, A.; Yargeau, V.; Szkopek, T. Selective ion sensing with high resolution large area graphene field effect transistor arrays. *Nature Communications* **2020**, *11* (1), 1-12.

(10) Berchmans, S.; Issa, T. B.; Singh, P. Determination of inorganic phosphate by electroanalytical methods: A review. *Analytica Chimica Acta* **2012**, *729*, 7-20.

(11) Martín Várguez, P. E.; Brunel, F.; Raimundo, J. M. Recent Electrochemical/Electrical Microfabricated Sensor Devices for Ionic and Polyionic Analytes. *ACS Applied Materials and Interfaces* **2020**.

(12) Gieling, T. H.; van Straten, G.; Janssen, H. J. J.; Wouters, H. ISE and Chemfet sensors in greenhouse cultivation. *Sensors and Actuators B: Chemical* **2005**, *105* (1), 74-80. DOI: 10.1016/j.snb.2004.02.045.

(13) Chaniotakis, N. A.; Alifragis, Y.; Konstantinidis, G.; Georgakilas, A. Gallium nitride-based potentiometric anion sensor. *Analytical Chemistry* **2004**, *76* (18), 5552-5556. DOI: 10.1021/ac049476h.

(14) Sherbow, T. J.; Kuhl, G. M.; Lindquist, G. A.; Levine, J. D.; Pluth, M. D.; Johnson, D. W.; Fontenot, S. A. Hydrosulfide-selective ChemFETs for aqueous H2S/HS− measurement. *Sensing and Bio-Sensing Research* **2021**, *31*, 100394-100394. DOI: 10.1016/j.sbsr.2020.100394.

(15) Abdel-Haleem, F. M.; Rizk, M. S. Development of ionophore-based nanosphere emulsion incorporating ion-exchanger for complexometric titration of thiocyanate anion. *Journal of Advanced Research* **2017**, *8* (4), 449-454. DOI: 10.1016/j.jare.2017.06.005.

(16) Antonisse, M. M. G.; Reinhoudt, D. N. Potentiometric anion selective sensors. *Electroanalysis* **1999**, *11* (14), 1035-1048.

(17) Bobacka, J.; Ivaska, A.; Lewenstam, A. Potentiometric ion sensors. *Chemical Reviews* **2008**, *108* (2), 329-351.

(18) Kaisti, M. Detection principles of biological and chemical FET sensors. *Biosensors and Bioelectronics* **2017**, *98* (June), 437-448.

(19) Mikhelson, K. N.; Peshkova, M. A. Russian chemical reviews. *Nature* **1960**, *188* (4749), 453-453.

(20) Crespo, G. A. Recent Advances in Ion-selective membrane electrodes for in situ environmental water analysis. *Electrochimica Acta* **2017**, *245*, 1023-1034.

(21) Moschou, E. A.; Chaniotakis, N. A. Chemfet based microsensors covered with ion-partitioning polymeric membranes. *Mikrochimica Acta* **2001**, *136* (3-4), 205-209.

(22) Lee, C. S.; Kyu Kim, S.; Kim, M. Ion-sensitive field-effect transistor for biological sensing. *Sensors* **2009**, *9* (9), 7111-7131. DOI: 10.3390/s90907111. Bakker, E.; Bühlmann, P.; Pretsch, E. The phase-boundary potential model. *Talanta* **2004**, *63* (1), 3-20.

(23) Seah, G. E. K. K.; Tan, A. Y. X.; Neo, Z. H.; Lim, J. Y. C.; Goh, S. S. Halogen Bonding Ionophore for Potentiometric Iodide Sensing. *Analytical Chemistry* **2021**, *93* (46), 15543-15549.

(24) Havel, V.; Svec, J.; Wimmerova, M.; Dusek, M.; Pojarova, M.; Sindelar, V. Bambus[n]urils: A new family of macrocyclic anion receptors. *Organic Letters* **2011**, *13* (15), 4000-4003.

(25) Havel, V.; Babiak, M.; Sindelar, V. Modulation of Bambusuril Anion Affinity in Water. *Chemistry - A European Journal* **2017**, *23* (37), 8963-8968.

(26) Havel, V.; Sadilová, T.; Šindelář, V. Unsubstituted Bambusurils: Post-Macrocyclization Modification of Versatile Intermediates. *ACS Omega* **2018**, *3* (4), 4657-4663.

(27) Svec, J.; Dusek, M.; Fejfarova, K.; Stacko, P.; Klán, P.; Kaifer, A. E.; Li, W.; Hudeckova, E.; Sindelar, V. Anion-free bambus[6]uril and its supramolecular properties. *Chemistry - A European Journal* **2011**, *17* (20), 5605-5612.

(28) Itterheimová, P.; Bobacka, J.; Šindelář, V.; Lubal, P. Perchlorate Solid-Contact Ion-Selective Electrode Based on Dodecabenzylbambus[6]uril. *Chemosensors* **2022**, *10* (3), 1-16.

(29) Neal, J. F.; Saha, A.; Zerkle, M. M.; Zhao, W.; Rogers, M. M.; Flood, A. H.; Allen, H. C. Molecular Recognition and Hydration Energy Mismatch Combine to Inform Ion Binding Selectivity at Aqueous Interfaces. *Journal of Physical Chemistry A* **2020**, *124* (49), 10171-10180.

(30) Wojciechowski, K.; Linek, K. Anion selectivity at the aqueous/polymeric membrane interface: A streaming current study of potentiometric Hofmeister effect. *Electrochimica Acta* **2012**, *71*, 159-165.

(31) Xie, W. J.; Gao, Y. Q. A simple theory for the hofmeister series. *Journal of Physical Chemistry Letters* **2013**, *4* (24), 4247-4252. DOI: 10.1021/jz402072g. Kang, B.; Tang, H.; Zhao, Z.; Song, S. Hofmeister Series: Insights of Ion Specificity from Amphiphilic Assembly and Interface Property. *ACS Omega* **2020**, *5* (12), 6229-6239.

(32) Gibb, C. L. D.; Oertling, E. E.; Velaga, S.; Gibb, B. C. Thermodynamic Profiles of Salt Effects on a Host-Guest System: New Insight into the Hofmeister Effect. *Journal of Physical Chemistry B* **2015**, *119* (17), 5624-5638.

(33) Wojciechowski, K.; Kucharek, M.; Wróblewski, W.; Warszyński, P. On the origin of the Hofmeister effect in anion-selective potentiometric electrodes with tetraalkylammonium salts. *Journal of Electroanalytical Chemistry* **2010**, *638* (2), 204-211.

(34) Vail, S. L.; Barker, R. H.; Mennitt, P. G. Formation and Identification of cis- and traras-Dihydroxyimidazolidinones from Ureas and Glyoxal. *Journal of Organic Chemistry* **1965**, *30* (7), 2179-2182. DOI: 10.1021/jo01018a015.

(35) Fargher, H. A.; Sherbow, T. J.; Haley, M. M.; Johnson, D. W.; Pluth, M. D. C-H-S hydrogen bonding interactions. *Chemical Society Reviews* **2022**, *51* (4), 1454-1469.

(36) Fiala, T.; Sleziakova, K.; Marsalek, K.; Salvadori, K.; Sindelar, V. Thermodynamics of Halide Binding to a Neutral Bambusuril in Water and Organic Solvents. *Journal of Organic Chemistry* **2018**, *83* (4), 1903-1912.

(37) Lizal, T.; Sindelar, V. Bambusuril Anion Receptors. *Israel Journal of Chemistry* **2018**, *58* (3), 326-333.